DEUTSCHES ELEKTRONEN-SYNCHROTRON DESY

DESY 87-021
March 1987

PHYSICS AT HERA

by

R. Rückl

Deutsches Elektronen-Synchrotron DESY, Hamburg

ISSN 0418-9833

NOTKESTRASSE 85 · 2 HAMBURG 52

To be sure that your preprints are promptly included in the
HIGH ENERGY PHYSICS INDEX ,
send them to the following address (if possible by air mail) :

DESY
Bibliothek
Notkestrasse 85
2 Hamburg 52
Germany

DESY 87-021
March 1987

ISSN 0418-9833

PHYSICS AT HERA

R. Rückl

Deutsches Elektronen-Synchrotron DESY, Hamburg, F.R. Germany

Talk presented at the ECFA-Workshop LEP 200, Aachen, F.R. Germany,
Sept 28 - Oct 1, 1986.

PHYSICS AT HERA

R. Rückl
Deutsches Elektronen-Synchrotron DESY, Hamburg, Germany

1. INTRODUCTION

The Hadron-Elektron-Ring-Anlage[1,2], called HERA, which is presently under construction at DESY will provide collisions of electrons and positrons with protons in an unexplored energy range. The available beam energies will be

$$E_e \simeq (10\text{-}30)\ \text{GeV}$$
$$E_p \simeq (300\text{-}820)\ \text{GeV} \qquad (1)$$

yielding the total $e^{\mp}p$ centre-of-mass energy

$$\sqrt{s} = 2\sqrt{E_e\, E_p} \simeq (110\text{-}314)\ \text{GeV}. \qquad (2)$$

HERA will thus exceed the highest c.m. energy of present-day lepton scattering on fixed targets, that is $\sqrt{s} = \sqrt{2E_\mu m_p} \simeq 23$ GeV, by more than one order of magnitude. A similar factor of ten is gained in lepton-nucleon momentum transfer. At HERA practicable rates of events should be obtained up to values of

$$Q = \sqrt{4E_e\, E_l' \cos^2\theta_l/2} \simeq 200\ \text{GeV} \qquad (3)$$

where E_l' and θ_l denote the final lepton energy and scattering angle (relative to the p-beam direction), respectively. For comparison, fixed-target experiments have explored the range $Q < 20$ GeV. As for every collider, the actual virtue of HERA will much depend on the luminosity. The aim is

$$\mathcal{L} = (1\text{-}2) \times 10^{31}\ \text{cm}^{-2}\ \text{sec}^{-1}. \qquad (4)$$

Furthermore, design studies[3] of systems of spin rotators indicate that it should be possible to turn the transverse polarization of the electrons (and positrons) which at $E_e \simeq 30$ GeV is building up in approximately half an hour, into longitudinal polarization. The maximum degree of polarization attainable is roughly

$$P_{L,R} \simeq 80\ \% \qquad (5)$$

for both left- and right-handedness. This greatly improves and extends the experimental possibilities at HERA since the helicity states $e^{+}_{L,R}$ all have different weak interactions with protons. For technical details of the HERA project and status reports one may consult, for example, Refs. 1-3.

Experimentation at HERA is scheduled to begin in 1990. Two large detectors, H1 and ZEUS, are presently being built. The H1-Collaboration has been joined by about 170

physicists from eight countries (France, FRG, GDR, Italy, Switzerland, UK, USA, USSR). The ZEUS-Collaboration with ~270 physicists from ten countries (Canada, FRG, Israel, Italy, Japan, Netherlands, Poland, Spain, UK, USA) is even bigger. For details about the detectors and their expected performance I refer to the original proposals[4,5]. However, I want to point out a peculiarity of ep collisions at HERA which has far-reaching consequences for the detector design and the possible measurements. Because of the much higher energy of the proton beam with respect to the e -beam, most of the final state particles fly in the direction of the incoming proton. This fact is illustrated in Fig. 1 for the case of deep-inelastic ep scattering as described in terms of the elementary processes eq → eq and eq → $\nu_e q'$ involving γ, Z and W exchange, respectively. The kinematics of ep → lX is basically fixed by the negative square Q^2 of the momentum of the exchanged vector boson and the momentum fraction x of the proton carried by the initial quark. Experimentally, these variables are determined from eq. (3) and the relations

$$x = \frac{Q^2}{ys} \quad , \quad y = 1 - \frac{E_l'}{E_e} \sin^2\theta_l/2 \tag{6}$$

by measuring the angle θ_l and the energy E_l' of the final electron in neutral current (NC) scattering processes. Relations similar to eqs. (3) and (6) hold for x, Q^2, y and the current-quark energy and scattering angle. Hence, by reconstructing the latter quantities from the observed current-jet one has an independent way of determining x, Q^2 and y. Obviously, in the charged current (CC) case, this is the only possible way. Both procedures put strong requirements on the detectors, in particular in the very forward direction and at large scattering angles as can be seen from Fig. 1. The expected precision in the x, Q^2 and y determination is discussed thoroughly in Refs. 4 and 5. On the whole, the topology of ordinary NC and CC events does not pose too big a problem and should permit a rather clear distinction of possible exotic events.

I now come to the main subject of my talk, the physics at HERA. The spectrum of possible investigations is quite remarkable. Below I give a fairly detailed but certainly not complete list of topics:

(A) strong interaction physics

- proton structure and quark/gluon densities
- QCD scaling violations and running of α_s
- properties of structure functions such as longitudinal SF, sum rules, behaviour at very small x
- jets and energy flow
- single particle inclusive production
- low Q^2 photoproduction
- QED/QCD Compton scattering
- heavy quark (in particular top) and quarkonium production

(B) electroweak interaction physics

- structure of neutral and charged weak currents
- W and Z properties
- 1-loop effects

(C) possible new physics

- new weak bosons and currents
- non-standard (pseudo-) scalar bosons
- leptoquarks
- supersymmetric particles
- compositeness of leptons and quarks

Quite evidently, the physics which can be investigated at HERA is in various respects complementary to the physics at LEP 200, the latter being discussed at the present Workshop. For example, HERA experiments will be capable of measuring quark and gluon densities in a wide range of x and Q^2 and putting QCD to systematic and stringent tests. On the other hand, precision measurements of W properties and also the search for the Higgs boson at LEP 200 would permit unique tests of the standard electroweak theory. Furthermore, the existence of new particles and interactions is probed by very different processes in ep and e^+e^- collisions providing thus experimentally independent evidence or constraints. This is most obvious in the case of new weak bosons and leptoquarks. To conclude this short introduction with a trivial statement, both HERA and LEP 200 have unique capabilities. An adequate comparison is therefore difficult, if not impossible.

In this talk I can of course not exhaust the physics possibilities at HERA. Since I was asked to emphasize those topics which are also studied at this workshop from the point of view of LEP 200, I decided to concentrate on the examples of new physics mentioned in category (C) of the list given above. However, before entering this discussion I want to make at least a few remarks also on the standard physics case. In preparing this talk I have greatly profitted from earlier reports[6-10] on the physics of ep-collisions. Many of the aspects and details which I will have to omit can be found there.

2. STANDARD PHYSICS

The various processes which can take place in ep collisions may be classified in

(a) low Q^2 photoproduction,
(b) high Q^2 NC and CC scattering,
(c) production of heavy quarks,
(d) production of Z and W bosons,
(e) Higgs boson production.

The scattering of almost real photons off protons represents by itself a rich field of HERA physics. Interesting measurements[11,12] include the total γp cross section, elastic Compton scattering ($\gamma p \rightarrow \gamma p$), diffractive production of vector mesons ($\gamma p \rightarrow Vp$) and, most notably, high p_T jet and single particle production. The latter re-

actions have proven[13] remarkably efficient in testing the basic QED/QCD processes,

$$\gamma q \longrightarrow \gamma q/gq \text{ and } \gamma g \longrightarrow q\bar{q}\ , \tag{7}$$

and even higher order effects in present-day fixed-target experiments at $E_\gamma^{Lab} \simeq 100$ GeV. In comparison, the HERA γp c.m. energy for a 10 GeV photon radiated off a 30 GeV electron and colliding with a 820 GeV proton corresponds to $E_\gamma^{Lab} \simeq 17$ TeV! Given the high γp energies,

$$\sqrt{s_{\gamma p}} \simeq (130\text{-}260) \text{ GeV for } E_\gamma \simeq (5\text{-}20) \text{ GeV and } E_p \simeq 820 \text{ GeV}, \tag{8}$$

the sizeable effective luminosity[11],

$$\mathcal{L}_{\gamma p} \simeq 10^{-2}\mathcal{L}_{ep} \simeq 10^{29} \text{ cm}^{-2} \text{ sec}^{-1} \text{ for } \theta_e \sim (10\text{-}100)\text{mrad}, \tag{9}$$

and the comfortably large cross sections[12] such as

$$\sigma(\gamma p \longrightarrow gX) \simeq 10 \text{ nb for } E_\gamma \simeq 15 \text{ GeV and } p_T^g > 2 \text{ GeV}, \tag{10}$$

it will be possible to study in great detail the hadronic nature of the photon, its point-like behaviour and perturbative QCD.

Yet, the main physics interest clearly concentrates on the processes (b)-(e) of the above list. Relative to low Q^2 photoproduction, these processes are generally quite rare. Nevertheless, as shown in Table 1, the expected event rates are reasonable to comfortable in most cases. The estimates involve various approximations which are discussed in the quoted literature. Some comments are in order.

Among the most important tasks of HERA is the study of proton structure and of QCD. In fact, the deep-inelastic structure functions $F_i(x,Q^2)$, i=1,2,3 are very appropriate observables for a systematic test of QCD[14] through the pattern of scaling violations, for the accurate determination of the running coupling constant $\alpha_s(Q^2)$ and finally for the precise measurement of quark densities and, less directly, of the gluon density as well. These structure functions are directly obtained from the inclusive ep cross sections. For example, in the NC case one has[8]

$$\frac{d\sigma(e^{\mp}p)}{dx\,dQ^2} = \frac{4\pi\alpha^2}{xQ^4}\left[y^2 x F_1(x,Q^2) + (1-y)F_2(x,Q^2) \pm \left(y-\frac{y^2}{2}\right) x F_3(x,Q^2)\right] \tag{11}$$

where, in leading order QCD,

$$\begin{aligned} F_2(x,Q^2) = 2xF_1(x,Q^2) &= \sum_f A_f(Q^2) \times \left[q_f(x,Q^2) + \bar{q}_f(x,Q^2)\right] \\ xF_3(x,Q^2) &= \sum_f B_f(Q^2) \times \left[q_f(x,Q^2) - \bar{q}_f(x,Q^2)\right] \end{aligned} \tag{12}$$

with q_f and $\bar{q}_f$ denoting quark and antiquark densities of flavor f, respectively. Further-

Table 1

Estimates of representative event rates at $\sqrt{s}$ = 314 GeV for an integrated luminosity $\int \mathcal{L}\,dt$ = 200 pb^{-1}

processes	dominant subprocesses	specifications	number of events	
$e^-p \to \nu_e X_h$	$e^-q \to \nu_e q'$	all Q^2	11250	a)
		$Q^2 > 10^4$ GeV^2	880	
$e^-p \to e^-X_h$	$e^-q \to e^-q$	$Q^2 > 10^3$ GeV^2	44660	
		$Q^2 > 10^4$ GeV^2	790	
$ep \to et\bar{t}X_h$	$\gamma g \to t\bar{t}$	m_t = 50 GeV	120	b)
$ep \to eZX_h$	$e\gamma \to eZ$	m_W = 83 GeV	7	c)
	$\gamma q \to Zq$		36	
$ep \to eWX_h$	$\gamma q \to Wq'$	m_Z = 93.8 GeV	154	
$ep \to \nu_e WX_h$	$e\gamma \to \nu_e W$	$\sin^2\theta_w$ = 0.217	3	
$ep \to eHX_h$	$WW \to H$	m_H = 50 GeV	2	d)

a) ZEUS-Collaboration, The ZEUS Detector-Technical Proposal (1986)

b) M. Drees and K. Grassie, Z. Phys. C28, 451 (1985)

c) E. Gabrielli, Mod. Phys. Lett. A1, 465 (1986)

d) G. Altarelli, B. Mele and R. Pitolli, Roma preprint 531 (1986)

more,

$$A_f(Q^2) = Q_f^2 - 2Q_f v_e v_f \frac{Q^2}{Q^2+m_Z^2} + (v_e^2+a_e^2)(v_f^2+a_f^2)\left(\frac{Q^2}{Q^2+m_Z^2}\right)^2$$

$$B_f(Q^2) = -2Q_f a_e a_f \frac{Q^2}{Q^2+m_Z^2} + 4 v_e v_f a_e a_f \left(\frac{Q^2}{Q^2+m_Z^2}\right)^2 \qquad (13)$$

where Q_f, v_f and a_f are the electromagnetic charges and the NC vector and axialvector couplings, respectively, with the convention Q_e = -1 and a_e = -1/2 $\sin^2\theta_w$. Similarly, the CC cross sections are given by

$$\frac{d\sigma(e^-p)}{dx\,dQ^2} = \frac{\pi\alpha^2}{4\sin^4\theta_w\,(Q^2+m_W^2)^2}\sum_{i,j}\Big[\,|V_{u_i d_j}|^2\,u_i(x,Q^2) + (1-y)^2\,|V_{u_j d_i}|^2\,\bar{d}_i(x,Q^2)\Big] \tag{14}$$

and $d\sigma(e^+p) \equiv d\sigma(e^-p;\ u_i,\bar{d}_i \rightarrow \bar{u}_i,d_i)$, where i is a family index and the V's denote elements of the Kobayashi-Maskawa matrix. The background to QCD scaling violations in $F_i(x,Q^2)$ from target mass and size effects, heavy flavor thresholds, higher twist operators and jet fragmentation etc. is still the main uncertainty in all quantitative QCD tests[15] at present energies and values of Q^2. These non-perturbative hadronic effects are expected to disappear with increasing Q^2 much faster than the calculable QCD scaling violations. Although the latter being determined by $\alpha_s(Q^2)$ also become smaller at high values of Q^2, one sees from Fig. 2 that the effect is clearly visible at HERA[7,16]. The influence of systematic uncertainties still remains to be seen. Careful consideration must further be given to the complications due to the W and Z propagators and the electroweak charges in Eqs. (12)-(14), to the effects of electroweak radiative corrections[17] and to thresholds (b,t,...) which may be crossed. I should also mention the exciting possibility of unveiling a substructure of electrons and quarks by studying the structure functions at the largest accessible values of Q^2. Note that at HERA one can penetrate to distances as small as $r \sim 1/Q \sim 10^{-16}$ cm and probe the existence of new physics even at scales $\Lambda \gg Q$ as illustrated later.

Testing the electroweak sector of the standard model[18] is another important task for HERA experiments. Through deep-inelastic e^+p scattering one can simultaneously study the structure of the charged and neutral weak currents and the W and Z propagators. When the momentum transfer reaches values of $Q \sim O(m_{W,Z})$, the electromagnetic and weak interactions become equally strong as indicated in Table 1 by the similar numbers of CC and NC events at $Q > 100$ GeV. In fact, the cross section for $ep \rightarrow eX$ is already sensitive to contributions from the Z boson at considerably lower values of Q^2, say $Q^2 > 1000$ GeV^2, so that the shape in Q^2 of the NC/CC ratio $\sigma(ep \rightarrow eX)/\sigma(ep \rightarrow \nu_e X)$ can serve as a suitable measure of electroweak parameters[19]. Moreover, with longitudinally polarized e^+ beams one can directly test the pure left-handed nature of the standard CC interactions by checking that $\sigma^{CC}(e_R^-p) = \sigma^{CC}(e_L^+p) = 0$. Longitudinal polarization also provides further handles on the neutral weak sector through the polarization asymmetries $A(e_L^- - e_R^-)$ and $A(e_L^+ - e_R^+)$, the charge asymmetries $A(e_L^- - e_L^+)$ and $A(e_R^- - e_R^+)$, and the mixed asymmetries $A(e_L^- - e_R^+)$ and $A(e_R^- - e_L^+)$. In the above,

$$A(e_1 - e_2) = \frac{\sigma(e_1) - \sigma(e_2)}{\sigma(e_1) + \sigma(e_2)} \tag{15}$$

where $\sigma(e_i)$ denote differential or (partly) integrated NC cross sections. These asymmetries have several virtues: they are large in the Q^2 range of HERA, very sensitive to the NC parameters and, in comparison to cross sections, less affected by uncertainties in the knowledge of quark densities. An example is shown in Fig. 3 where the polarization asymme-

try $A(e_L^- - e_R^-)$ integrated over x is plotted versus Q^2. Also indicated are the sensitivity to variations of $\sin^2\theta_w$ and the statistical errors corresponding to a run of 150 pb^{-1}. After a few years of running and a careful analysis of structure functions, scaling violations and electroweak radiative corrections, one can expect quite accurate tests of both NC and CC properties. Studies which will make this assertion more quantitative are on the way and will be presented at the DESY Workshop on Physics at HERA in fall 1987.

I have pointed out, several times, the importance of the electroweak radiative corrections. A thorough discussion of this difficult subject lies totally beyond the scope of my talk. However, I at least want to mention a recent study[17] of the problem and present some indicative numerical results. From Fig. 4 one can infer the pure QED and the weak part of the total radiative corrections to the differential $e^-p \longrightarrow e^-X$ cross section. The QED contributions are mainly due to vertex corrections and bremsstrahlung and are by far dominant. The weak corrections are small and dominated by the Z self energy. The total correction at x = 0.5 amounts to approximately - 40 %. Furthermore, it is very interesting to note large cancellations of the radiative corrections in the asymmetries defined in Eq. (15). Fig. 5 shows the remaining corrections to $A(e_L^- - e_R^-)$ which amount to less than about 10 %. In particular, $A(e_L^- - e_L^+)$ is almost unaffected by radiative corrections and, hence, a favorable observable for $\sin^2\theta_w$ determination. In the numerical calculations exemplified in Figs. 4 and 5 the following set of parameters has been used: $\alpha = 1/137$, $m_Z = 93$ GeV, $m_W = 82$ GeV (if not stated otherwise), $m_H = 100$ GeV, m_l from Ref. 20, m(u,d,s,c,b,t) = (0.03, 0.03, 0.15, 1.5, 4.5, 30) GeV and set I of the scaling violating parton distribution of Ref. 21. Furthermore, $\sin^2\theta_w = 1 - m_W^2/m_Z^2$ to all orders. The dependence on m_H and m_t is rather weak and probably not observable. For example, at x=y=0.5 $\delta A(e_L^- - e_R^-) \simeq 0.01$ and -0.02 for $m_H = 100 \longrightarrow 1000$ GeV and $m_t = 40 \longrightarrow 100$ GeV, respectively. Finally, I should not omit to say that the results of Ref. 17 disagree with earlier studies[22] so that this chapter is not yet closed.

Apart from NC and CC scattering, the production of W, Z[23-25] and Higgs bosons[26,27] is of principal interest. The main production mechanisms in ep collisions can be read off from Table 1. For a run of 200 pb^{-1} one predicts[24] a total of about 160 $W^{\pm}$ and 40 Z bosons. Although these rates are not overwhelming, they may also not be completely useless if the W and Z bosons can be reconstructed from their hadronic decays. It has not yet been studied in detail whether or not such a reconstruction is experimentally feasible. At any rate, the leptonic decays $W \longrightarrow e\nu_e$ and $Z \longrightarrow \nu\bar{\nu}$ with the branching ratios $B(W \longrightarrow e\nu_e) \simeq 0.083$ and $B(Z \longrightarrow \nu_e\bar{\nu}_e + \nu_\mu\bar{\nu}_\mu + \nu_\tau\bar{\nu}_\tau) \simeq 0.19$ represent a non-negligible background to missing energy signals from possible new physics such as the production of supersymmetric particles[23]. On the other hand, concerning the standard neutral Higgsboson H^0 HERA experiments will have little to say. Here, the dominant mechanism is WW-fusion. ZZ-fusion is less efficient by a factor of 7, while $\gamma\gamma$ production involving virtual loops can be totally neglected. Thus, not too surprisingly, the production cross section is extremely small in the HERA energy range, giving[26] 6-1 H^0's per 200 pb^{-1} for m_H = (10-60) GeV. However, the existence of non-standard (maybe charged) scalars or pseudoscalars with masses accessible at HERA and considerably larger couplings is not yet excluded and worth some consideration[27].

I shall finish this very brief and only indicative account of standard physics at HERA with some remarks on heavy quark production. The number of $c\bar{c}$ and $b\bar{b}$ pairs produced via γg-fusion is substantial[11]. A small fraction of these pairs form quarkonium resonances. Particularly noteworthy is the case of inelastic J/ψ production[28] in $\gamma g \to J/\psi g$ as it provides[29] a direct measurement of the gluon density in the proton at $x \cong O(10^{-3})$. Also top quarks can be produced with appreciable rates. According to the estimates of Ref. 30, one expects $\sim 600(25)$ $ep \to e t\bar{t} X$ events for $m_t = 40(60)$ GeV and an integrated luminosity of 200 pb^{-1}. The decays of these heavy quarks lead to a burst of many particles in the direction of the incoming proton, isotropically distributed in the plane perpendicular to the beams. Hence, it should not be too difficult to distinguish $t\bar{t}$ events from other processes[2]. This invites one to some speculations. Top search at the CERN $p\bar{p}$-collider[31] has shown that it is very non-trivial to detect top production at hadron machines. Very light top quarks with $m_t < 30$ GeV would be a case for TRISTAN. If $m_t < 50$ GeV, clear evidence should come from SLC and LEP I. However, if the top quark is just a little bit heavier than 50 GeV, top may actually be discovered at HERA! Finally, in case $m_t < m_W$ top would also be seen in W decays at LEP 200.

3. NEW PHYSICS POSSIBILITIES

There is no experimental result that unquestionably contradicts the standard model. However, it has serious theoretical deficiencies as evident from the large number of unexplained structural features and parameters. Well-known questions concern the dynamical origin and the values of the particle masses, the understanding of why there are several (maybe exactly three) families of fermions, flavor mixing and parity violation in weak interactions, and finally, the unification of the fundamental forces. Also the presence of an elementary Higgs boson in the standard theory is somewhat problematic and certainly lacking in experimental confirmation. Attempts to solve these problems have produced many interesting ideas of possible physics beyond the standard model.

Generally, the energy scale of such new physics is rather high. This is either required by the phenomenological success of the standard model which makes it difficult to modify it or to add something new, or it simply reflects the natural scale of the problem considered. Some of the proposed ideas and the typical scales involved are indicated below:

- left-right symmetric extensions of the electroweak model[32]: $m_{W_R} \gtrsim O(1\ \text{TeV})$
- composite Higgs boson as envisaged in technicolor theories[33]: $\Lambda_{TC} \lesssim O(1\ \text{TeV})$
- composite leptons and quarks, and composite models of weak bosons[34,35]: $\Lambda \gtrsim O(1\ \text{TeV})$
- composite models of families[35], and horizontal symmetries[36]: $\Lambda \gtrsim O(100\ \text{TeV})$
- supersymmetry as a solution of the gauge hierarchy problem[37]: $m(\text{SUSY particles}) \lesssim O(1\ \text{TeV})$
- grand unification[38]: $\Lambda \sim O(10^{15}\ \text{GeV})$
- supergravity[37], and superstring[39]: $\Lambda \gtrsim 10^{19}$ GeV.

Admittedly, I have dropped many clever proposals from this list such as the composite Higgs models discussed in Ref. 40, the strongly coupled standard models considered in Ref. 41, and others. While physics at $\Lambda \lesssim O(10\ \text{TeV})$ is within the reach of the new colliders coming into operation or now being built, future e^+e^- and pp supercolliders will give access to $\Lambda \lesssim O(100\ \text{TeV})$. On the other hand, experimental tests of grand unification and

and superstring theories seem extremely difficult, at least at accelerators.

All of the above models raise new questions and problems which are far from being solved. This situation and the, in some cases, enormous extrapolations in scale render predictions for phenomena at collider energies rather uncertain. With this caution in mind, I shall now illustrate the physics reach of HERA. Sections 3.1-3.3 deal with new interactions detectable by measuring inclusive cross sections and asymmetries, while the production of new particles and some typical signatures are considered in sections 3.4-3.6. The examples discussed are representative for new physics searches at HERA, but in no way exhaustive. Many other exotic processes have been contemplated in the literature in connection with HERA. Moreover, the experiments may have surprises in store for us.

3.1. Superstring-motivated Z'

Superstring theories[39] represent an important step towards a "theory of everything" that in the low energy limit comprises the so successful standard model. Although it is still rather mysterious how superstrings in higher dimensions above the Planck scale may be linked to the effective particles and interactions relevant at collider energies, superstring-inspired phenomenology has already become a common topic of physics studies for future machines.

One such superstring-motivated conjecture[42] is the existence of a new neutral boson Z' with $m_{Z'} \lesssim O(1\ \text{TeV})$. Roughly speaking, compactification of the heterotic $E_8 \times E_8$ superstring in 10 dimensions on suitable Calabi-Yau manifolds may yield a supersymmetric E_6 grand-unified theory in 4 dimensions with the E_6 symmetry broken by the Wilson loop mechanism at the Planck scale to some subgroup G of E_6. In case there is no further symmetry breaking at intermediate scales and G is the low energy group, it must necessarily be bigger than the standard gauge group. This leaves

$$G = SU(3)_C \times SU(2)_L \times U(1)_Y \times U(1)_{Y'} \subset E_6 \tag{16}$$

as the minimal low energy theory containing the standard model.

The electroweak sector of (16) contains, besides the photon and the standard weak bosons, a new neutral boson Z' associated with $U(1)_{Y'}$. Furthermore, the 15 helicity components of a standard fermion family form, together with new fermion species, a fundamental 27-plet of E_6. The fields and quantum numbers of the lightest family are specified in Table 2. Corresponding assignments are assumed for the heavier families. Note that the electromagnetic charge obeys the usual relation $Q_{em} = T_3 + Y$ where T_3 is the third component of the weak isospin. Finally, the Higgs fields also belong to a 27-plet of E_6 so that all of them are $SU(2)_L$ doublets or singlets. The supersymmetric counterparts of the above degrees of freedom play no role for the present discussion and are, therefore, not considered further.

In order to provide masses to all weak bosons, the $SU(2)_L \times U(1)_Y \times U(1)_{Y'}$ symmetry must be broken spontaneously to $U(1)_{em}$. The neutral mass eigenstates Z_1 and Z_2 are in general mixtures of Z and Z',

$$Z_1 = \cos\theta\, Z + \sin\theta\, Z', \quad Z_2 = -\sin\theta\, Z + \cos\theta\, Z'. \tag{17}$$

Table 2

Multiplet structure and U(1) charges of a fermion 27-plet of E_6 in the model defined by Eq.(16)

E_6	SO(10)	SU(5)	$SU(3)_c$	$SU(2)_L$	Y	Y'	L-fields
27	16	10	3	2	1/6	1/3	u d
			$\bar{3}$	1	-2/3		u^c
			1	1	1		e^c
		$\bar{5}$	$\bar{3}$	1	1/3	-1/6	d^c
			1	2	-1/2		ν_e e
		1	1	1	0	5/6	N_e^c
	10	5	3	1	-1/3	-2/3	h
			1	2	1/2		E^c N_E^c
		$\bar{5}$	$\bar{3}$	1	1/3	-1/6	h^c
			1	2	-1/2		ν_E E
	1	1	1	1	0	5/6	n

Evidently, the lower mass eigenstate Z_1 is to be indentified with the already observed neutral weak boson. While in the absence of mixing m_{Z_1} coincides with the standard model value m_Z, Eq. (17) implies

$$m_Z^2 = \cos^2\theta\, m_{Z_1}^2 + \sin^2\theta\, m_{Z_2}^2 \geq m_{Z_1}^2 . \tag{18}$$

Furthermore, the familiar W-Z mass relation of the standard model is replaced by

$$\varrho = \frac{m_W^2}{m_Z^2 \cos^2\theta_W} = 1 \tag{19}$$

with m_Z^2 given by Eq. (18). Hence, as a second consequence of mixing, the Weinberg angle θ_W defined by the gauge couplings, $\sin^2\theta_W = g_Y^2/(g_L^2 + g_Y^2)$, or equivalently by Eq. (19) differs from the angle $\bar{\theta}_W$ obtained from the W and Z_1 mass ratio:

$$\sin^2\bar{\theta}_W = 1 - \frac{m_W^2}{m_{Z_1}^2} \leqslant 1 - \frac{m_W^2}{m_Z^2} = \sin^2\theta_W . \qquad (20)$$

Thirdly, because of mixing the couplings of Z_1 to the ordinary fermions deviate from the standard NC couplings. Evidence for the presence of a second neutral boson can thus arise indirectly from modifications of the standard NC phenomenology due to mixing as well as directly from new processes involving Z_2.

Altogether, the neutral current sector of the above model depends on five parameters: m_{Z_1}, m_{Z_2}, θ, θ_W, and the $U(1)_Y$, gauge coupling $g_{Y'}$. These are treated as follows. According to the conjecture that the two U(1) factors of (16) break down at comparable scales, one takes $g_{Y'} = g_Y = e/\cos\theta_W$. Furthermore, m_{Z_1} is assumed to be fixed by experiment. The nominal value substituted in later numerical estimates for HERA is $m_{Z_1} = 93.3$ GeV. Using then Eq. (19) and[43] $m_W = 38.65\ \text{GeV}/\sin\theta_W$ one can determine the Weinberg angle θ_W as a function of m_{Z_2} and θ. Lastly, m_{Z_2} and θ being related to unknown Higgs expectation values are considered as essentially free parameters.

Present-day bounds[44-47] on Z_2 come from low-energy neutral current data, W and Z mass measurements, and from the negative result of the Z' searches at the CERN Collider. The allowed domain in (m_{Z_2}, θ) is exhibited in Fig. 6. One sees that the present lower limit on the Z_2 mass is rather weak: $m_{Z_2} \gtrsim 150$ GeV. This is not too surprising considering the relatively small value of the gauge coupling $g_{Y'}$. Future experiments at the FNAL Tevatron, SLC and LEP can be expected to give access to considerably heavier masses: $m_{Z_2} \lesssim 230$ GeV in $\bar{p}p$ collisions[48] at 2 TeV and $m_{Z_2} \lesssim 500$ GeV in e^+e^- collision[49] on the Z peak.

The weak coupling of Z_2 to ordinary fermions makes the case[49,50] also somewhat difficult for HERA. Here, one has to search for deviations from the standard model expectations in NC processes $ep \longrightarrow eX$ at large Q^2. As pointed out in chapter 2 asymmetry measurements with longitudinally polarized $e^{\mp}$ -beams are particularly powerful for electroweak tests. Fig. 6 illustrates the sensitivity to the presence of Z_2 for three representative asymmetries defined in Eq. (15). Shown are the contours in (m_{Z_2}, θ) for which the standard model asymmetries A(Z) and the asymmetries $A(Z_1,Z_2)$ predicted by the two-Z model differ by $\delta A = |A(Z_1,Z_2) - A(Z)| = 0.04$ at $x = 0.3$ and $Q^2 = 2\times10^4$ GeV^2. Preliminary studies indicate that effects of this size may be detectable by a careful analysis of the Q^2-dependence (see e.g. Fig. 3), provided that the degree of polarization is not much lower than about 80 %. Further interesting results[50] are summarized below:

(1) The various asymmetries differ greatly in sensitivity to Z_2 (see Fig. 6).

(2) The effects on a given asymmetry depend on details of the model considered (see e.g. section 3.2).

(3) The domain in (m_{Z_2}, θ) where the changes δA of the asymmetries mainly come from Z_2-exchange (flat parts of the contours in Fig. 6 at relatively small values of m_{Z_2} and θ) is clearly distinguishable from the regions where the effects dominantly originate in Z-Z' mixing (steep parts of the contours at large values of m_{Z_2} and $\theta \neq 0$).

These observations emphasize how important it is to study as many asymmetries as possible in order to optimize the detection limits, to distinguish the existence of a new gauge boson Z_2 from other possible sources of an effect which might be seen, and to determine some detailed properties of Z_2. Unfortunately, such a comprehensive measurement has also a serious drawback, namely the sharing of luminosity among $e^{\pm}_{L,R}p$ collisions. One must therefore find some reasonable compromise. In summary, if no deviation from the standard model predictions on asymmetries is observed at HERA it should be possible to put the following constraints on the parameters of the superstring-motivated Z_2 boson associated with (16):

$$m_{Z_2} \gtrsim 300 \text{ GeV and } |\theta| \lesssim 2^\circ . \tag{21}$$

On the other hand, if a signal is seen it will be difficult to attribute it unambiguously to the existence of Z_2, unless m_{Z_2} is considerably smaller than the value (21).

3.2. Left-Right Symmetry

Left-right symmetric models [32] are motivated by the attempt to understand P and C violations in weak interactions. The general idea is to begin with a P and C conserving electroweak Lagrangian, and to attribute the observed P and C violations to the non-invariance of the vacuum.

The simplest L-R symmetric extension of the standard $SU(2)_L \times U(1)_Y$ theory is based on the group

$$SU(2)_L \times SU(2)_R \times U(1)_{B-L} , \tag{22}$$

with a discrete L-R symmetry so that $g_L = g_R$ where $g_{L,R}$ are the $SU(2)_{L,R}$ gauge couplings. One now has a second isotriplet of gauge fields $\vec{W}_R$ associated with $SU(2)_R$, and the right-handed leptons (including ν_R) and quarks which are $SU(2)_L$ singlets become doublets under $SU(2)_R$. The complete assignment of leptons and quarks thus reads as follows:

$$\begin{aligned} l_L &= (1/2,\ 0,\ -1)\ ,\ l_R = (0,\ 1/2,\ -1)\ , \\ q_L &= (1/2,\ 0,\ 1/3)\ ,\ q_R = (0,\ 1/2,\ 1/3). \end{aligned} \tag{23}$$

The electromagnetic charge is given by $Q = T_{3L} + T_{3R} + \frac{B-L}{2}$ with the difference of baryon (B) and lepton (L) number playing the role of the U(1) charge. Due to spontaneous symmetry breaking all gauge bosons, but the photon eventually acquire masses. While the charged mass eigenstates $W^{\pm}_{1,2}$ are mixtures of $W^{\pm}_{L,R}$ ($g_L = g_R = e/\sin\theta_w$; $J^{\pm}_{L,R}$), the neutral mass eigenstates $Z_{1,2}$ can be represented as mixtures of the standard Z and a new Z' boson with the following couplings and currents: $g_Z = g_{Z'} = e/\sin\theta_w\cos\theta_w$ and $J_Z = J_{3L} - \sin^2\theta_w J_{em}$, $J_{Z'} = (\cos^2\theta_w J_{3R} + \sin^2\theta_w (J_{3L} - J_{em}))/\sqrt{\cos 2\theta_w}$. The respective mixing angles are denoted by ξ and θ and the convention is as in Eq. (17). Deviations from standard model parameters and relations due to mixing have been pointed out in 3.1. Again, the lower mass eigenstates $W^{\pm}_1$ and Z_1 are identified with the observed weak bosons. Following the strategy adopted in 3.1, one may treat the heavier masses m_{W_2} and m_{Z_2} and the mixing angles ξ and θ as free phenomenological parameters. Theoretically, these parameters are determined by

the Higgs boson structure. In addition, one has a new K-M matrix which describes flavor mixing in the right-handed currents $J_R^{\pm}$ and which is, in the simplest models, the same or the charge conjugate of the left K-M matrix. Let me first consider the neutral current sector of the above L-R model. The observed W and Z mass values together with low-energy NC data imply[44,45,51] $m_{Z_2} \gtrsim 300$ GeV and θ less than a few degrees. More definite limits are depicted in Fig. 7 where the Higgs constraint (19) has been used. This Figure further illustrates the deviations of the polarization asymmetry $A(e_L^- - e_R^-)$ from the standard model value $A(Z) = 0.35$ at $x = 0.3$ and $Q^2 = 2\times10^4$ GeV^2 in NC scattering at HERA, and the variation of the effects with m_{Z_2} and θ. The remarks made at the end of section 3.1 in connection with Fig. 6 also apply to the present case. Moreover, I want to emphasize the different shape of the contours in Fig. 7 as compared to Fig. 6, that is the sensitivity of asymmetries to details of the models. The most stringent tests[52] of the existence of the heavy neutral boson Z_2 associated with the simplest left-right symmetric extension of the standard electroweak theory are provided by the polarization asymmetries $A(e_L^+ - e_R^+)$ and the charge asymmetry $A(e_R^- - e_R^+)$. With a similar experimental precision as the one leading to the detection limit (21) for a neutral E_6 boson, one would have access to masses of Z_2 in the range

$$m_{Z_2} \lesssim (500 - 700) \text{ GeV}. \tag{24}$$

The charged current sector of (22) provides an interesting example for heavy W searches at HERA. The constraints[44] on W_2 and right-handed currents resulting from present-day CC phenomenology depend on the processes considered (μ and β decays, non-leptonic decays, K_L-K_S mass difference, ν scattering etc.) and on various model assumptions (m_{ν_R}, q_R mixing etc.). The mass bounds range from $m_{W_2} > 300$ GeV to 4 TeV, while W_L-W_R mixing must be small in any case: $|\zeta| < (0.3\text{-}5)^0$. Thus, the existence of charged $SU(2)_R$ bosons with masses in the few hundred GeV range cannot yet be ruled out, although there are indications that W_R must be searched for in the TeV region. The relevant W_R-exchange process in ep collisions is $eq \longrightarrow \nu_R q'$ where the right-handed neutrino could be light or heavy, and it could be a Dirac or Majorana fermion. Fig. 8 shows the expected cross sections for two indicative cases: $m_{\nu_R} \simeq 0$ and $m_{\nu_R} \simeq m_{W_R}$. The mixing angle ζ is assumed to vanish. In the theoretically preferred case[32], that is for a heavy Majorana neutrino, the cross section is rather discouraging:

$$\sigma(ep \longrightarrow \nu_R X) \simeq 0.01 \text{ pb for } m_{\nu_R} = m_{W_R} \simeq 200 \text{ GeV}. \tag{25}$$

On the other hand, the signature would be spectacular: $\nu_R \longrightarrow e^-X$ and e^+X with equal branching fractions. Conversely, for a light Dirac neutrino the cross section is more comfortable:

$$\sigma(ep \longrightarrow \nu_R X) \simeq 0.1 \text{ pb for } m_{\nu_R} = 0,\ m_{W_R} \simeq 500 \text{ GeV}. \tag{26}$$

However, the clear $e^{\pm}$-signal is now not available, and one must therefore search for small right-handed current contributions to inclusive CC scattering. This is another case where

longitudinal polarization is extremely important for detection. Unfortunately, even for 80 % polarization the background from ordinary left-handed weak interactions is substantial. It has been estimated[16] that for an integrated luminosity of $\sim 250\ pb^{-1}$ shared between the two e^- polarizations and for $G_R^{cc}/G_L^{cc} \simeq 0.02$ at $Q^2 > 5000\ GeV^2$, a cross section ratio expected for $m_{W_R} \simeq 300$ GeV, one would just observe a 3σ effect. This indicates that inclusive searches for right-handed currents in the mass range

$$m_{W_R} \lesssim 500\ GeV \tag{27}$$

demand very high polarization and long running times.

3.3. Residual interactions

Attempts to solve the flavor and mass problems of the standard model have led to the suggestion that quarks and leptons may be composite of more elementary constituents.[34,35] The binding force should probably be confining at a scale $\Lambda \gtrsim O(1\ TeV)$ so that the bound state radius would be characterized by $r \sim 1/\Lambda \lesssim O(10^{-17}\,cm)$. Hence, $m_{l,q} \ll O(\Lambda) \sim 1/r$ quite in contrast to our experiences with ordinary QCD bound states such as the ρ meson or the nucleon. Notwithstanding the above and other puzzles of this approach, it is interesting to study how this conjecture could be checked experimentally. Clearly, at energies $E > \Lambda$ the composite nature of leptons and quarks should become manifest. However, one would also expect some observable effects at energies $E < \Lambda$. An essentially unavoidable consequence of compositeness are residual interactions[53,54] induced by the strong binding force. Such interactions are described by non-renormalizable operators in the effective low-energy Lagrangian. The most important of these are four-fermion operators which have dimension 6 and, therefore, dimensionful coupling constants: g^2/Λ^2. As the binding force is most likely strong, one may plausibly take $g^2/4\pi = 1$. These contact interactions interfer with the conventional gauge interaction and yield deviations of order $Q^2/\alpha\,\Lambda^2$ from the standard model expectations. Here, Q^2 is the typical scale of a process and α is one of the usual gauge couplings. Since $\alpha \ll 1$ these effects are already observable at $Q^2 \ll \Lambda^2$. In fact, from Bhabha scattering[55] at PETRA and PEP one has derived limits $\Lambda_{ee} > 1\text{-}3$ TeV for various assumptions on the chiral form of the contact terms, while high p_T jet production at the CERN Collider[56] has provided the bound $\Lambda_{qq} > 450$ GeV.

In ep collisions, one can test lepton-quark contact interactions and bound the scale parameter Λ_{eq}. For definiteness, I restrict myself to the NC processes $eq \longrightarrow eq$ using the effective Lagrangian[57]

$$\mathcal{L}_{eff} = g^2 \Big[\frac{\eta_{LL}}{\Lambda_{LL}^2} (\bar{e}_L \gamma^\mu e_L)(\bar{q}_L \gamma_\mu q_L) + \frac{\eta_{LR}}{\Lambda_{LR}^2} (\bar{e}_L \gamma^\mu e_L)(\bar{q}_R \gamma_\mu q_R) + \frac{\eta_{RL}}{\Lambda_{RL}^2} (\bar{e}_R \gamma^\mu e_R)(\bar{q}_L \gamma_\mu q_L) + \frac{\eta_{RR}}{\Lambda_{RR}^2} (\bar{e}_R \gamma^\mu e_R)(\bar{q}_R \gamma_\mu q_R) \Big] \tag{28}$$

where the coefficients η_{ab} take the values ± 1 or 0, and $g^2/4\pi = 1$. The following cases are considered: VV($\eta_{LL} = \eta_{LR} = \eta_{RL} = \eta_{RR}$), AA($\eta_{LL} = -\eta_{LR} = -\eta_{RL} = \eta_{RR}$),

LL($\eta_{LR} = \eta_{RL} = \eta_{RR} = 0$) and, correspondingly, LR, RL, RR. Fig. 9 shows the effects of a LL contact term on the differential cross section $d\sigma(e^-p \to e^-X)/dQ^2$ for various values of Λ_{LL}. For an integrated luminosity of 200 pb^{-1} one should be sensitive to $\Lambda_{LL} \simeq 5$ TeV as indicated by the statistical errors.

Similarly as in the case of new gauge bosons studied in 3.1 and 3.2, asymmetries[57] are very useful for testing the helicity structure of the effective interactions in (28). This is illustrated in Fig. 10 where the polarization asymmetry $A(e_L^- - e_R^-)$ is plotted for all models defined above and for $\Lambda_{ab} = 3$ TeV in comparison with the standard model prediction. As can be seen, $A(e_L^- - e_R^-)$ is particularly sensitive to LL and RR contact interactions. Table 3 summarizes the results of a comprehensive study[57] of all asymmetries defined in Eq. (15) and their sensitivity to Λ_{ab} for each helicity combination considered in Fig. 10. From this Table one can infer the most sensitive asymmetry for a given contact

Table 3

Survey of the sensitivity of asymmetries to contact interactions
(at $x = 0.3$, $Q^2 = 2\times10^4$ GeV^2)

helicity structure of contact term	most sensitive asymmetry A	standard model value of A	Λ_{eq}(TeV) for $\delta A = 0.08$	Λ_{eq}(TeV) for $\delta A = 0.04$
LL	$e_L^- - e_R^-$	0.35	4	5
LR	$e_R^- - e_R^+$	0.17	5	7
RL	$e_L^+ - e_R^+$	-0.38	7	10
RR	$e_L^- - e_R^-$	0.35	5	7
VV	$e_L^- - e_L^+$	0.73	5	7
AA	$e_R^- - e_R^+$	0.17	6.5	9

term (in some cases there are several asymmetries with comparable sensitivity), the standard model values of these asymmetries at $x = 0.3$ and $Q^2 = 2\times10^4$ GeV^2, and the values of Λ_{ab} for which these asymmetries deviate from the standard model prediction by $\delta A = 0.04$ and 0.08. One can conclude from this analysis that asymmetry measurements at HERA could probe eq contact interactions up to compositeness scales Λ_{eq} in the range

$$\Lambda_{eq} \simeq (5 - 10) \text{ TeV}, \tag{29}$$

provided that the precision also assumed for (21) and (24) is achieved.

3.4. Excited leptons and quarks

Composite models for the known leptons and quarks also predict many excited states[34,35] with both conventional and exotic quantum numbers. Naively, one would expect $m^* \sim O(\Lambda)$ for the masses of these particles where Λ is the compositeness scale. As $\Lambda \gtrsim O(1\ \text{TeV})$ this would preclude production at HERA. However, it is possible that the same mechanism which keeps the ground state fermions light also leads to some relatively light excited states. Experimentally, at least, this possibility is not excluded. For example, searches for excited electrons in e^+e^- annihilation at PETRA put the mass limit[55] $m_{e^*} > (23 - 70)$ GeV where the smaller number is independent of the coupling strength of excited to ground state electrons.

For illustration of the capabilities at HERA for the production and detection of excited leptons, I shall consider the case[7,9,58] of a weak isospin doublet ($\nu^* e^*$). The most important process is single inclusive production $ep \rightarrow l^* X$ involving el^*V-transitions where $V = \gamma$, Z and W. Gauge invariance requires a magnetic-type coupling, while possible problems with (g-2) measurements are avoided if this coupling is restricted to one helicity component of the electron. The effective Lagrangian can then be written in the form[58]

$$\mathcal{L}_{eff} = \sum_{V=\gamma,Z,W} c_{el^*V} \frac{e}{\Lambda} \bar{l}^* \sigma^{\mu\nu} e_L \partial_\mu V_\nu + h.c. \qquad (30)$$

where the coefficients c_{el^*V} specify the relative coupling strengths to γ, Z and W, the conventions being $c_{ee^*\gamma} = -(f + f')/2$ and $c_{e\nu^*W} = f/\sqrt{2}\sin\theta_W$. The inclusive cross sections for e^* and ν^* production are shown in Fig. 11 as a function of the heavy lepton mass. Note that elastic e^* production, $ep \rightarrow e^* p$, amounts to about 50 % of the total e^* cross section which receives the dominant contribution from photon exchange at low Q^2. Furthermore, the decay $e^* \rightarrow e\gamma$ provides a very clean signature[9]: a peak in the invariant mass distribution of $e\gamma$ pairs above a manageable background and a jet of hadrons or, even more strikingly, a single proton in the extreme forward direction. Hence, 10 events per 100 pb^{-1} may be sufficient for detection. In that case, one can probe the existence of excited electrons with couplings $f/\Lambda = f'/\Lambda \simeq 1\ \text{TeV}^{-1}$ up to masses

$$m_{e^*} \simeq 200\ \text{GeV} \qquad (31)$$

as can be seen from Fig. 11. On the other hand, the prospects of detecting excited neutrinos are less promising because of the smaller production rate and the perhaps more complicated decay modes such as $\nu^* \rightarrow eW$, $W \rightarrow \nu l$ or $q\bar{q}'$.

Similar rates as far as the e^* are expected for excited quark production[59] at the hadronic vertex, $ep \rightarrow eq^* X$, if one assumes an effective qq^*V coupling corresponding to (30). However, the signature[9] from the supposedly dominant decay mode $q^* \rightarrow qg$ is less striking and the background due to conventional processes such as $\gamma q \rightarrow gq$ and $\gamma g \rightarrow q\bar{q}$ is more severe. Finally, most composite models contain also more exotic boundstates such as color-octet leptons or color-sextet quarks. Searches for such states at HERA are discussed for example, in Ref. 60.

3.5. Leptoquarks

In the standard model leptons and quarks enter as independent fields. On the other hand, their electromagnetic charges are quantized in the same units, their weak SU(2) properties are identical and also their family structure matches. This strongly suggests that in a more fundamental theory leptons and quarks should be interrelated and, correspondingly, new particles should exist which mediate lepton-quark transitions. Such states are generically called leptoquarks (LQ) and occur naturally in superstring models[61] and grand-unified theories[38], but also in technicolor theories[9,33] and models of quark-lepton substructure[34,35,41].

One can distinguish various kinds of leptoquarks with spin and $SU(3)_c \times SU(2)_L \times U(1)_Y$ quantum numbers as given below:

(A) LQ's coupled to lepton-quark channels:
$(3,1,-1/3 \text{ or } -4/3)_{J=0}$, $(3,3,-1/3)_{J=0}$, $(3,2,-5/6 \text{ or } 1/6)_{J=1}$;

(B) LQ's coupled to lepton-antiquark channels:
$(3^*,2,7/6 \text{ or } 1/6)_{J=0}$, $(3^*,3,2/3)_{J=1}$, $(3^*,1,2/3 \text{ or } 5/3)_{J=1}$.

The electric charges are $Q = T_3 + Y = 2/3$, $-1/3$ or $-4/3$ for class (A) and $5/3$, $2/3$ or $-1/3$ for class (B). Furthermore, in some theories such as technicolor and composite models global symmetry breaking gives rise to J=0 leptoquarks which are pseudo-Goldstone bosons. In this case, the couplings to fermion pairs are proportional to the fermion masses. Finally, leptoquarks violating baryon and lepton number must be extremely heavy in order to avoid rapid proton decay, while those with baryon and lepton number conserving couplings have to satisfy only much weaker bounds[62]. In particular, low-energy experiments permit the existence of leptoquarks with flavor-diagonal couplings as large as electroweak gauge couplings (but only to either left- or right-handed leptons) and with masses of order 100 GeV.

Such low mass leptoquarks could be produced at HERA. In fact, as leptoquarks are per definitionem resonances in eq channels an ep collider such as HERA is an ideal machine to search for them[61,63,64]. A systematic study of all possible scalar and vector leptoquarks has been performed in Ref. 63. Here, I concentrate on the $(3,1,-1/3)_{J=0}$ leptoquark S_1 which couples to the e^-u and $\nu_e d$ channels and which is assumed to be not a pseudo-Goldstone boson. Using the effective Lagrangian[63]

$$\mathcal{L}_{eff} = g_{1L} (\bar{u}^c d^c)_L \, i\tau_2 \begin{pmatrix} \nu_e \\ e \end{pmatrix}_L S_1 + h.c. \qquad (32)$$

with $\psi^c = C \bar{\psi}^T$ being a charge conjugated fermion field, one readily obtains for the total S_1 width

$$\Gamma_{S_1} = \frac{g_{1L}^2}{8\pi} m_{S_1} \simeq 0.7 \text{ GeV} \qquad (33)$$

where $g_{1L} = 0.3 \simeq e$ and $m_{S_1} = 200$ GeV has been used. Thus, leptoquarks accessible at HERA will be very narrow. The cross sections for the fusion processes $e^-u \rightarrow S_1$ and $e^+\bar{u} \rightarrow \bar{S}_1$ are also easily calculated from (32):

$$\sigma(e^{\mp}p \rightarrow S_1 X) = f\,\frac{\pi^2\alpha}{s}\,\bar{u}^{(-)}\left(\frac{m_{S_1}^2}{s}\,,\,m_{S_1}^2\right) \qquad (34)$$

where $\bar{u}(x,Q^2)$ are the up- und antiup-quark densities, respectively, and $f\alpha = g_{1L}^2/4\pi$. Fig. 12 shows the resonance cross sections (34) as a function of m_{S_1} for f = 0.1-1. One sees that present bounds allow copious production of leptoquarks at HERA. For f=1 and m_{S_1} = 250 GeV one expects 4000 events per 200 pb^{-1}! Conversely, leptoquarks with $m_{S_1} \simeq$ 200 GeV can be discovered for 30 times smaller couplings g_{1L}, that is for f = 10^{-3}!

Although the subsequent S_1 decays, $S_1 \rightarrow e$ or ν_e + jet yield events which at first sight look like conventional NC and CC events, the angular distributions[64] of the decay leptons and jets are very different from the normal distributions (see also Fig. 1). Moreover, the inclusive y distribution of leptoquark events is flat, in contrast to the falling distributions from normal NC and CC scattering. Therefore, it should be rather easy to detect a possible leptoquark signal. The clearest evidence for leptoquarks would be narrow peaks in the inclusive x-distributions centred at $x = m_{LQ}^2/s$. These peaks should become clearly visible after applying a cut in Q^2 (or y), e.g. $Q^2 > 10^4$ GeV^2, in order to suppress the NC and CC background. This is illustrated in Fig. 13 where results of a complete calculation[63] are shown including the standard processes and all interference effects with s- and u-channel S_1 exchange. Of course, in a real experiment the very narrow peaks in Fig. 13 would be smeared out by the finite resolution in x. Nevertheless, the above estimates indicate that leptoquarks with couplings $g_{LQ}^2/4\pi \sim O(\alpha)$ are detectable at HERA up to masses very close to the phase space boundary:

$$m_{LQ} \simeq (250\text{-}300)\ \text{GeV}. \qquad (35)$$

The possibility to probe the existence of leptoquarks with $m_{LQ} > \sqrt{s} = 314$ GeV exists also. Such heavy leptoquarks induce effective four-fermion interactions similar to the ones discussed in 3.3 and thus give rise to indirect signals in inclusive CC and NC cross sections and asymmetries[63,64]. From the expected sensitivity to the compositeness scale Λ_{eq} detailed in 3.3, one can estimate the maximum values of m_{LQ} accessible to such indirect tests:

$$m_{LQ} \sim \sqrt{f\alpha}\,\Lambda_{eq} < \sqrt{f}\ 500\ \text{GeV}. \qquad (36)$$

Taking f=1 and comparing (36) with (35) one sees that if no effect is observed the direct mass limit (35) can be improved by roughly a factor of two.

As a final remark, leptoquarks which are pseudo-Goldstone bosons have sizeable couplings only to heavy fermions or gauge bosons and are, therefore, more difficult to produce in ep collisions. Dominant mechanisms are expected to be $e + g(\rightarrow \bar{t}t) \rightarrow LQ + t$ and $\gamma + g \rightarrow LQ + LQ$. Substituting for the relative coupling strength f introduced earlier essentially $f \sim \varepsilon^2 m_t^2/m_W^2$ as suggested in the technicolor framework[33] and taking m_t = 50 GeV, one estimates[65] a LQ yield from electron-gluon fusion of about 800 ε^2 events per 200 pb^{-1} for $m_{LQ} \simeq$ 150 GeV at maximum HERA energy. Here ε denotes an unknown mixing

angle. The anticipated decay modes $LQ \longrightarrow l\bar{t}$ with $l = e,\mu,\tau$ followed by heavy flavor decays lead to final states which provide plenty of signatures[9] such as isolated muons and heavy quark jets containing further leptons. These can quite efficiently be separated from the background[9,66] of conventional photoproduction and deep-inelastic processes including $ep \longrightarrow et\bar{t}+X$. Thus, leptoquark Goldstone bosons can be studied in the interesting[33] mass range $m_{LQ} \simeq 150$ GeV, provided that f is as assumed above and $\varepsilon^2 > 0.1$. The unknown mixing parameter ε does not enter in leptoquark pair production via photon-gluon fusion. However, the production rate being of the same order as the one for top quarks given in Table 1 is only significant for $m_{LQ} \lesssim$ (50-60) GeV.

3.6. Supersymmetry

Besides being an interesting and elegant mathematical construction, supersymmetry may play a profound role in particle physics. Indications for that are provided by supergravity and superstring theories. Moreover, SUSY may be of immediate importance for the standard model by protecting the mass parameters of the elementary Higgs sector from quadratically divergent radiative shifts and stabilizing the Fermi scale[37]. If the socalled naturalness problem of the standard model is solved in this way the supersymmetric partners of the conventional particles must have masses in the range $\tilde{m} \lesssim O(1\ \text{TeV})$.

The minimal supersymmetric extension of the standard model[37,67] predicts the following superpartners:

(A) sleptons and squarks (s=o): $\tilde{l}_{L,R}$, $\tilde{q}_{L,R}$
(B) gauginos (s = 1/2): $\tilde{g}$, $\tilde{\gamma}$, $\tilde{Z}$, $\tilde{W}^{\pm}$
(C) higgsinos (s = 1/2): $\tilde{H}^{o}$, $\tilde{H}^{o\prime}$, $\tilde{H}^{\pm}$

Note also that this model has at least two scalar Higgs doublets. The couplings of the above weak eigenstates are fixed by gauge invariance and supersymmetry. After SUSY breaking, the physical fields which acquire masses are mixtures of the weak eigenstates. Since the SUSY breaking mechanism is not really known, both the masses and mixing angles are uncertain. However, models[37] exist which predict the mass spectrum and the mixing from renormalization group equations in terms of a few breaking parameters such as genuine gaugino and scalar masses. In the usual supersymmetric theories, there is also a discrete symmetry, called R-parity, which is multiplicatively conserved and distinguishes ordinary particles (R = +1) from their superpartners (R = -1). This has two important phenomenological consequances: firstly, SUSY particles can be produced only in pairs and, secondly, the lightest sparticle being stable escapes detection and thus causes imbalance of energy and momentum. Mass limits for SUSY particles have been obtained from searches at the CERN $p\bar{p}$ Collider and in e^+e^- annihilation at PETRA and PEP. The results depend on the assumed mass relations and decay modes. The least model-dependent bounds are $m_{\tilde{l}} > 20$ GeV, $m_{\tilde{W}} > 20$ GeV (e^+e^- experiments[55]) and $m_{\tilde{q}} \gtrsim 70$ GeV, $m_{\tilde{g}} \gtrsim 60$ GeV (preliminary UA1 result[68]). However, the situation presumably changes before HERA comes into operation. While squarks and gluino masses in the range $m_{\tilde{q}}$, $m_{\tilde{g}} \lesssim$ (120,150) GeV are expected to be probed at the FNAL Tevatron[69], one should be able to discover sleptons and winos at LEP[70] if $m_{\tilde{l}}$, $m_{\tilde{W}} \lesssim 50$ GeV.

The main source of SUSY particles in ep collisions is the associated production of

- sleptons and squarks[71-73]: $eq \longrightarrow \tilde{e}\tilde{q}$ and $\tilde{\nu}\tilde{q}'$,

- sfermions and gauginos[74]: $e\gamma \to \tilde{e}\tilde{\gamma}$, $\tilde{\nu}\tilde{W}$ etc., and
- squarks and gluinos[30,71]: $\gamma g \to \tilde{q}\bar{\tilde{q}}$ and $\gamma q \to \tilde{g}\tilde{q}$.

Furthermore, the existence of squarks and gluinos would affect the running of $\alpha_s(Q^2)$ at $Q^2 \gg m_{\tilde{q}}^2$, $m_{\tilde{g}}^2$ and also change the properties of the deep-inelastic structure functions[71,75] essentially through the evolution of $\tilde{q}$ and $\tilde{g}$ densities inside the proton. However, in the light of the already existing mass bounds one finds that slepton-squark production is by far the most promising SUSY process to be searched for at HERA. Therefore, I shall discuss here only the latter one.

The relevant diagrams are depicted in Fig. 14. In order to calculate the corresponding cross sections[71-73] one has first to diagonalize the $(\tilde{W}^+, \tilde{H}^+)$ and $(\tilde{\gamma}\ \tilde{Z}\ \tilde{H}^0\ \tilde{H}^{0\prime})$ mass matrices[67] which involve four unknown quantities: the mass parameters M_1, M_2 and M_H associated with the $U(1)_Y$ and $SU(2)_L$ gauginos and the higgsinos, respectively, and the ratio v_2/v_1 of the vacuum expectation values of the two Higgs scalars. The problem becomes more manageable if one makes the reasonable assumptions that $M_1 \simeq M_2$ at the grand-unification scale and that $v_1 \simeq v_2$, and if M_1, M_2 and M_H are taken to be real. Furthermore, it is very convenient for phenomenological applications to determine the chargino ($\chi_i^\pm$, i = 1,2) and neutralino (χ_i^0, i = 1,2,3,4) mass eigenstates and their mass values in terms of the lightest chargino and neutralino masses. This procedure has been chosen in Ref. 73. Three representative solutions are given in Table 4. Fig. 14 shows the corresponding cross sections at the highest HERA energy which, in a large range of $\tilde{l}$ and $\tilde{q}$ masses, depend only on

Table 4

Chargino and neutralino masses (GeV) and corresponding mass eigenstates characterized by the $(\tilde{W}^+, \tilde{H}^+)$ and $(\tilde{\gamma}, \tilde{Z}, \tilde{H}^0)$ admixtures (%), respectively, using $m_{\chi_1^\pm}$ and $m_{\chi_1^0}$ as input in the diagonalization procedure[a)]

	χ_1^{+-}	χ_2^{+-}	χ_1^0	χ_2^0	χ_3^0	$\chi_4^0 \equiv \tilde{H}^{0\prime}$
a	30 (88,12)	225 (12,88)	0 (100,0,0)	37 (0,86,14)	232 (0,14,86)	195 -
b	80 (34,66)	93 (66,34)	20 (99,0,1)	92 (0,37,63)	102 (1,63,36)	21 -
c	30 (4,96)	448 (96,4)	20 (2,7,91)	213 (80,15,5)	449 (18,78,4)	47 -

a) H. Komatsu and R. Rückl, DESY preprint in preparation.

the sum $m_{\tilde{l}} + m_{\tilde{q}}$. One sees that the production rates of sleptons and squarks are rather sensitive to gaugino mixing, that is in our approach to the masses $m_{\chi_1^\pm}$ and $m_{\chi_1^0}$ of the lightest gaugino mass eigenstates. The relative magnitude of the cross sections a to c in Fig. 14 can qualitatively be understood on the basis of the information given in Table 4. Requiring a minimum cross section of 0.1 pb for detection, which corresponds

to about 10 events per year, one finds the following theoretical detection limits:

$$m_{\tilde{e}} + m_{\tilde{q}} \lesssim 180 \text{ GeV (a)}, 170 \text{ GeV (b)}, 150 \text{ GeV (c)},$$
$$m_{\tilde{\nu}} + m_{\tilde{q}} \lesssim 170 \text{ GeV (a)}, 150 \text{ GeV (b)}, 160 \text{ GeV (c)} \qquad (37)$$

where a to c refers to the assumed gaugino system.

Whether or not the mass range (37) can be reached experimentally depends on the dominant decay modes of sleptons and squarks. Since the ratios of sparticle masses and, in particular, the supposedly stable sparticle are not precisely known, it is difficult to answer this question reliably. In the most favourable case where the photino is stable and $m_{\tilde{g}} > m_{\tilde{q}}$ so that $\tilde{e} \longrightarrow e\tilde{\gamma}$ and $\tilde{q} \longrightarrow q\tilde{\gamma}$, the answer is a cautious yes. This assertion is briefly substantiated below. Although the visible particles are the same in $ep \longrightarrow \tilde{e}\tilde{q}X \longrightarrow ej\tilde{\gamma}\tilde{\gamma}X$ as in conventional NC events, $ep \longrightarrow ejX$, the electron and jet momentum correlations present in NC scattering (see Fig. 1) is completely lost in SUSY events due to the escaping photinos. As a consequence, the values of the scaling variables x and y determined from the measured e momentum using Eq.(3,6)generally differ from the values of x and y obtained from a q-jet measurement, i.e. $\Delta x = x_q - x_e \neq 0$ and $\Delta y = y_q - y_e \neq 0$, whereas for NC events $\Delta x \simeq 0$ and $\Delta y \simeq 0$. This also applies to the difference $\Delta\varphi = \varphi_q - \varphi_e - \pi$ of the azimuthal angles. The MC simulations shown in Fig. 15 demonstrate convincingly that it should not be too difficult to separate signal and background. Indeed, more detailed studies[9] indicate that with cuts $|\Delta y| > 0.2$ and $|\Delta\varphi| > 0.2$ one can remove the NC background with less than 20 % loss in signal. Further significant backgrounds could arise from heavy flavor and weak boson decays[23] in processes such as $ep \longrightarrow et\bar{t}X$ and $ep \longrightarrow eWX$ [24] as can be seen from the rates given in Table 1. Such relatively rare processes should also be studied carefully. Finally, concerning the CC SUSY reaction $ep \longrightarrow \tilde{\nu}\tilde{q}X$; $\tilde{\nu} \longrightarrow \nu\tilde{\gamma}$, $\tilde{q} \longrightarrow j\tilde{\gamma}$ and also for more complicated $\tilde{l}$ and $\tilde{q}$ decay chains one may consult Ref. 9.

4. SUMMARY

HERA will provide ep collisions in a new energy range. In comparison to present-day fixed target lN scattering one will gain more than two orders of magnitude in equivalent lepton beam energy and one order of magnitude in usable lN momentum transfer: $E_l \simeq 50$ TeV and $Q_{max} \simeq 200$ GeV. Furthermore, there is a good chance for performing physical experiments with longitudinally polarized $e^{\pm}$ beams. This will make HERA to a flexible and powerful tool for the study of strong and electroweak physics.

I have briefly pointed out the many ways offered by HERA to put the standard model to stringent tests. Most noteworthy are

- the investigation of the proton structure, in particular, at high Q^2 and small x,
- the study of the running of α_s and the pattern of scaling violations of deep-inelastic structure functions in a large range of Q^2,
- the test of perturbative QCD in hard scattering processes, and
- the examination of the structure of neutral and charged weak currents, Z and W propagators and, to some extent, even of radiative effects.

A special topic of great interest is further top quark search in the mass range $m_t \lesssim 60$ GeV.

The main part of this talk has been devoted to searches for possible new physics. This subsubject is by nature very speculative. In order to facilitate a comparison with the physics reach of other machines (in particular, LEP200) I have selected examples which have become more or less standard for such purposes: heavy Z' and W' bosons and new weak currents, residual four-fermion interactions, excited fermions, leptoquarks and supersymmetric particles. These topics are also strongly motivated by theoretical perspectives on physics beyond the standard model. Keeping in mind that detection limits are very model-dependent and often not particularly well defined, one may characterize the bounds below which new physics can be probed at HERA as follows:

- neutral bosons (E_6 or $SU(2)_L \times SU(2)_R \times U(1)_{B-L}$)	$m_{Z'} \simeq$ (300 or 600) GeV
- charged bosons ($SU(2)_R$; $m_{\nu_R} \simeq m_{W_R}$ or 0)	$m_{W_R} \simeq$ (200 or 400) GeV
- electron-quark contact interactions	$\Lambda_{eq} \simeq$ (5-10) TeV
- excited electrons	$m_{e^*} \simeq 200$ GeV
- leptoquarks (pseudo-Goldstone bosons or not)	$m_{LQ} \simeq$ (150 or 300) GeV
- selectron and squarks	$m_{\tilde{e}} + m_{\tilde{q}} \simeq 180$ GeV.

In the first three examples (except in the case of a heavy Majorana neutrino) one is dealing with indirect signals. The physics source of such effects can be identified with some confidence only at lower masses and scales than the ones quoted.

Although HERA may not be comparable in precision with LEP as far as electroweak tests are concerned, or in available energy and luminosity with a hadron collider, it does have complementary virtues and unique capabilities. Among the topics discussed, these are the study of proton structure and QCD, including sensitive tests of substructure effects in eq collisions, and the search for new particles carrying the electron number in a mass range beyond LEP.

ACKNOWLEDGEMENTS

I want to thank my collaborators F. Cornet and H. Komatsu for numerous discussions on various subjects I have presented in this talk and for kindly providing Figs. 3,7,9,10 (F.C.) and Fig. 14 (H.K.).

REFERENCES

1) See, e.g. Reports at the 13. Int. Accelerator Conf., Novosibirsk, 1986, DESY M-86-10 (1986).

2) G. Wolf, Lectures at the Advanced Study Institute on Techniques and Concepts of High Energy Physics, St. Croix, Virgin Islands, 1986, DESY 86-089 (1986).

3) D.P. Barber, Talk at the 7. Int. Symp. on High Energy Spin Physics, Protvino, USSR, 1986, DESY 86-170 (1986).

4) H1 Collaboration, Technical Proposal for the H1 Detector (1986).

5) ZEUS Collaboration, The ZEUS Detector - Technical Proposal (1986).

6) Proc. of the Study of an ep Facility for Europe (ed. U. Amaldi), DESY 79/48 (1979) and Proc. of the Workshop Experimentation at HERA, DESY HERA 83/20 (1983).

7) G. Altarelli, B. Mele, and R. Rückl, in Proc. of the ECFA-CERN Workshop on Large Hadron Collider in the LEP Tunnel (ed. M. Jacob), CERN report 84-10 (1984), p. 551.

8) R. Rückl, in Proc. of the 13. Int. Winter Meeting on Fundamental Physics (ed. M. Aguilar-Benitez and A. Ferrando) (Instituto de Estudios Nucleares, Madrid, 1986), p. 288 and in the Quark Structure of Matter (ed. M. Jacob and K. Winter) (World Scientific Publ. Co., Singapore, 1986), p. 717.

9) R.J. Cashmore et al., Phys. Rep. 122, 275 (1985).

10) J.A. Bagger and M.E. Peskin, Phys. Rev. D31, 2211 (1985) and erratum.

11) W. Hoogland, in Proc. of the Study of an ep Facility for Europe (ed. U. Amaldi), DESY 79/48 (1979), p. 315.

12) J.J. Engelen, in Proc. of the Workshop Experimentation at HERA, DESY HERA 83/20 (1983), p. 241.

13) P. Aurenche et al., Phys. Lett. 135B, 164 (1984) and Z. Phys. C24, 309 (1984).

14) For a review see, e.g. G. Altarelli, Phys. Rep. 81, 1 (1982).

15) R. Voss, in The Quark Structure of Matter (ed. M. Jacob and K. Winter) (World Scientific Publ. Co., Singapore, 1986), p. 141; Ch. Geweniger, in DESY-Workshop: QCD - Theory and Phenomenology, Internal Report DESY T-86-01 (1986), p. 364.

16) E. Longo, in Proc. of the Workshop Experimentation at HERA, DESY HERA 83/20 (1983), p. 285.

17) M. Böhm and H. Spiesberger, University of Würzburg preprints (1986).

18) For a review see, e.g. H. Fritzsch and P. Minkowski, Phys. Rep. 73, 67 (1981).

19) J. Blümlein, M. Klein and T. Riemann, Akad. d. Wiss., Zeuthen, GDR, in preparation.

20) Particle Data Group, Phys. Lett. 170B, 1 (1986).

21) D.W. Duke and J.F. Owens, Phys. Rev. D30, 49 (1984).

22) J. Feltesse, in Proc. of the Workshop Experimentation at HERA, DESY HERA 83/20 (1983), p. 371.

23) G. Altarelli, G. Martinelli, B. Mele, and R. Rückl, Nucl. Phys. B262, 204 (1985).

24) E. Gabrielli, Mod. Phys. Lett. A1, 465 (1986).

25) A.N. Kamal, J.N. Ng and H.C. Lee, Phys. Rev. D24, 2842 (1981);
P. Salati and J.C. Wallet, Z. Phys. C16, 155 (1982);
H. Neufeld, Z. Phys. C17, 145 (1983);
M. Böhm and A. Rosado, University of Würzburg preprint (1987).

26) G. Altarelli, B. Mele and R. Pitolli, Roma preprint 531 (1987).

27) Z. Hioki, S. Midorikawa and H. Nishiura, Prog. Theor. Phys. 69, 1484 (1983);
J.A. Bagger and M.E. Peskin, Ref. 10;
D.A. Dicus and S.S.D. Willenbrock, Phys. Rev. D32, 1642 (1985);
R. Bates and J.N. Ng, Phys. Rev. D33, 657 (1986);
K.J.F. Gaemers, University of Amsterdam, private communication.

28) E.L. Berger and D. Jones, Phys. Rev. D23, 1521 (1981);
R. Baier and R. Rückl, Nucl. Phys. B201, 1 (1982) and B218, 289 (1983).

29) A.D. Martin, C.-K. Ng and W.J. Stirlin, University of Durham, DTP/87/6 (1987).

30) M. Dress and K. Grassie, Z. Phys. C28, 451 (1985).

31) M. Della Negra (UA1 Collaboration), in Proc. of the XV. Int. Symp. on Multiparticle Dynamics (ed. G. Gustafson and C. Peterson) (World Scientific Publ. Co., Singapore, 1984), p. 366.

32) For a review see, e.g. R.N. Mohapatra, in Quarks, Leptons and Beyond (ed. H. Fritzsch, R.D. Peccei, H. Saller and F. Wagner) (Plenum Press, New York, 1985), p. 219.

33) For a review see, e.g. E. Farhi and L. Susskind, Phys. Rep. 74, 277 (1981).

34) For reviews see, e.g. W. Buchmüller, Acta Phys. Austriaca Suppl. XXVII, 517 (1985);
M.E. Peskin, in Proc. of the 1985 Int. Symp. on Lepton and Photon Interactions at High Energies (ed. M. Konuma and K. Takahashi) (Kyoto University, Kyoto, 1986), p. 713.

35) See, for example, discussions by H. Harari, in Theory-Workshop: Physics at the Fermi Scale, Internal Report DESY T-85-02 (1985), p. 120;
R.D. Peccei, Lectures at the 17. Ecole d'Ete de Physique des Particules, Clermont Ferrand, France, 1985, DESY 86-010 (1986).

36) R.N. Cahn and H. Harari, Nucl. Phys. B176, 135 (1980) and references therein.

37) For reviews see, e.g. J. Ellis, in Proc. of the 1985 Int. Symp. on Lepton and Photon Interactions at High Energies (ed. M. Konuma and K. Takahashi) (Kyoto University, Kyoto, 1986), p. 850; H.P. Nilles, Phys. Rep. 110, 1 (1984).

38) For reviews see, e.g. P. Langacker, Phys. Rep. 72, 185 (1981) and in Proc. of the 1985 Int. Symp. on Lepton and Photon Interactions at High Energies (ed. M. Konuma and K. Takahashi) (Kyoto University, Kyoto, 1986), p. 186.

39) For reviews see, e.g. J.H. Schwarz, Phys. Rep. 89, 223 (1982) and Plenary Talk at the XXIII. Int. Conf. on High Energy Physics, Berkeley, 1986; M.B. Green, Surveys in High Energy Physics 3 (1983) 127.

40) See, for example, reviews by H. Georgi, in Proc. of the 1985 Les Houches Summer School; D.B. Kaplan, Talk at the XXIII. Int. Conf. on High Energy Physics, Berkeley, 1986.

41) L. Abbott and E. Farhi, Phys. Lett. 101B, 69 (1981) and Nucl. Phys. B189, 547 (1981);
M. Claudson, E. Farhi and R.L. Jaffe, Phys. Rev. D34, 873 (1986);
B. Schrempp, Talk at the 23. Int. Conf. on High Energy Physics, Berkeley, 1986, MPI-PAE/PTh 72/86 (1986) and references therein.

42) See, for example, review by R.D. Peccei, Plenary Talk at the XXIII. Int. Conf. on High Energy Physics, Berkeley, 1986, DESY 86-138 (1986) and references therein.

43) W.J. Marciano and A. Sirlin, Phys. Rev. D22, 2695 (1980).

44) P. Langacker, Ref. 38 (Kyoto Conference) and references therein.

45) L.S. Durkin and P. Langacker, Phys. Lett. 166B, 436 (1986).

46) V. Barger, N.G. Deshpande and K. Whisnant, Phys. Rev. Lett. 56, 30 (1986).

47) E. Cohen, J. Ellis, K. Enqqvist and D.V. Nanopoulos, Phys. Lett. 165B, 76 (1985);
J. Ellis, K. Enqvist, D.V. Nanopoulos and F. Zwirner, Nucl. Phys. 276B, 14 (1986).

48) M.J. Duncan and P. Langacker, Nucl. Phys. B277, 285 (1986).

49) V.D. Angelopoulos, J. Ellis, D.V. Nanopoulos and N.D. Tracas, Phys. Lett. 176, 203 (1986).

50) F. Cornet and R. Rückl., Phys. Lett. 184B, 263 (1987).

51) V. Barger, E. Ma and K. Whisnant, Phys. Rev. D26, 2378 (1982) and D28, 1618 (1983).

52) F. Cornet and R. Rückl, DESY preprint in preparation.

53) C.J.C. Burges and H.J. Schnitzer, Nucl. Phys. B228, 464 (1983) and Phys. Lett. 134B, 329 (1984); C.N. Leung, S.T. Love and S. Rao, Z. Phys. C31, 433 (1986);
W. Buchmüller and D. Wyler, Nucl. Phys. B268, 621 (1986).

54) E.J. Eichten, K.D. Kane and M.E. Peskin, Phys. Rev. Lett. 50, 811 (1983).

55) S. Komamiya, in Proc. of the 1985 Int. Symp. on Lepton and Photon Interactions at High Energies (ed. M. Konuma and K. Takahashi) (Kyoto University, Kyoto, 1986), p. 612.

56) C. Rubbia, ibid., p. 242.

57) R. Rückl., Phys. Lett. 129B, 363 (1983) and Nucl. Phys. B234, 91 (1984);
F. Cornet and R. Rückl, DESY preprint in preparation.

58) K. Hagiwara, D. Zeppenfeld and S. Komamiya, Z. Phys. C29, 115 (1985).

59) J.H. Kühn, H.D. Tholl and P.M. Zerwas, Phys. Lett. 158B, 270 (1985).

60) K.H. Streng, University of Munich preprint (1986);
T.G. Rizzo, Phys. Rev. D33, 1852 (1986) and D34, 133 (1986).

61) V.D. Angelopoulos et al., CERN-TH 4578/86 (1986); A. Dobado, M.J. Herrero and C. Munoz, University of Madrid, FTUAM/87-4 (1987).

62) W. Buchmüller and D. Wyler, Phys. Lett. 177B, 377 (1986).

63) W. Buchmüller, R. Rückl and D. Wyler, DESY 86-150 (1986).

64) J. Wudka, Phys. Lett. 167B, 337 (1986).

65) S. Rudaz and J.A.M. Vermaseren, CERN report TH-2961 (1981) and erratum.

66) P. Petiau, in The Quark Structure of Matter (ed. M. Jacob and K. Winter) (World Scientific Publ. Co., Singapore, 1986), p. 755;
D. Haidt, Internal DESY report H1-4/85-14 (1985).

67) H.E. Haber and G.L. Kane, Phys. Rep. 117, 75 (1985).

68) A. Homna, Talk at the XXIII. Int. Conf. on High Energy Physics, Berkeley, 1986;
see also E. Reya and D.P. Roy, Phys. Lett. 166B, 223 (1986).

69) H. Baer and E.L. Berger, Phys. Rev. D34, 1361 (1986); E. Reya and D.P. Roy, Z. Phys. C32, 615 (1987).

70) H. Baer et al., in Physics at LEP (ed. J. Ellis and R.D. Peccei), CERN 86-02, Volume 1 (1986), p. 297.

71) S.K. Jones and C.H. Llewellyn Smith, Nucl. Phys. B217, 145 (1983).

72) P.R. Harrison, Nucl. Phys. B249, 704 (1985).

73) H. Komatsu and R. Rückl, DESY preprint in preparation.

74) G. Altarelli et al., Ref. 23; P. Salati and J.C. Wallet, Phys. Lett. 122B, 397 (1983).

75) B.A. Campbell, J. Ellis and S. Rudaz, Nucl. Phys. B198, 1 (1982);
I. Antoniadis, C. Kounnas and R. Lacaze, Nucl. Phys. B211, 216 (1983);
C. Kounnas and D.A. Ross, Nucl. Phys. B214, 317 (1983);
L. Marleau, Phys. Rev. D32, 2928 (1985).

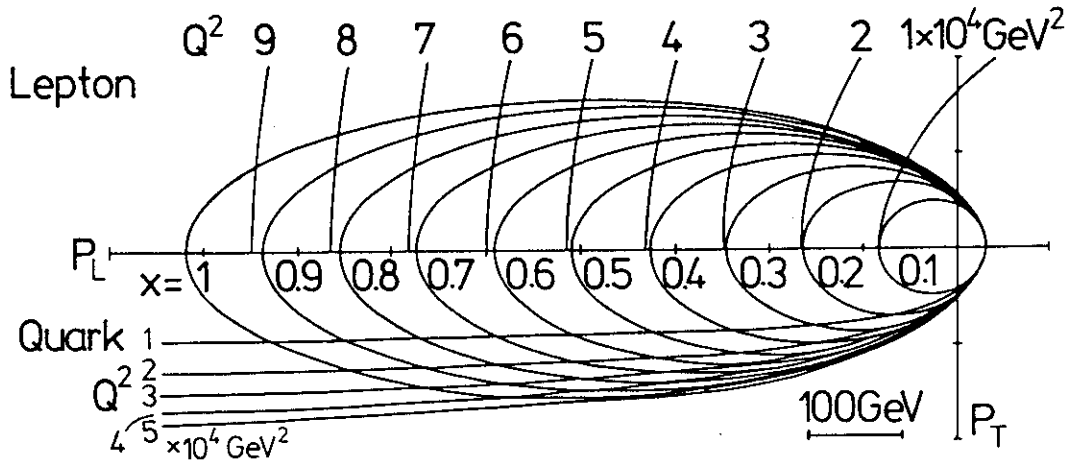

Fig. 1 Kinematics of the subprocess $eq \rightarrow lq'$ in collisions of 30 GeV electrons and 820 GeV protons[9]. An event is characterized by a point in (x,Q^2) on the lepton side and by the corresponding point on the quark side. The vectors joining the origin of the diagram with these points represent the momenta of the final lepton and quark-jet, respectively, in an event.

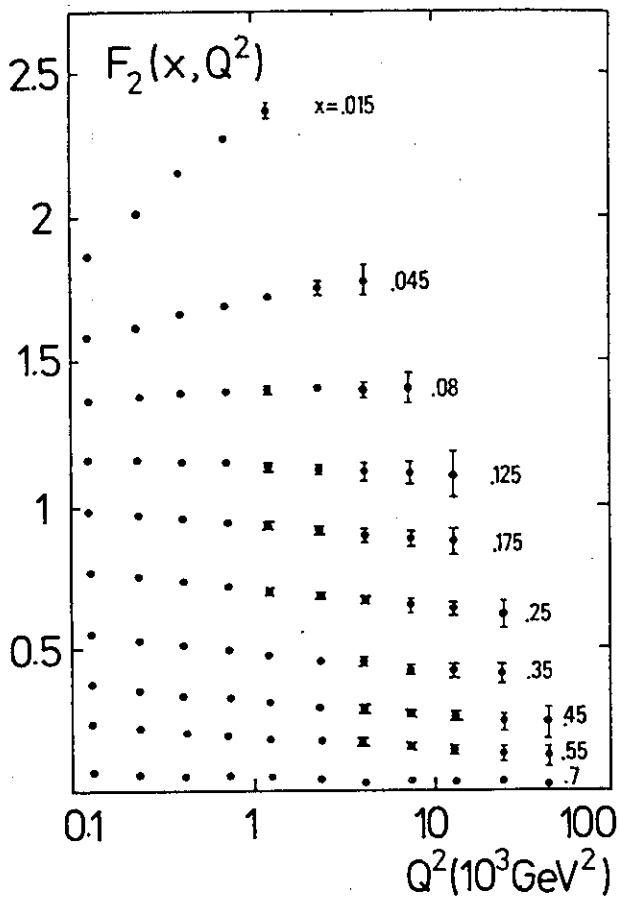

Fig. 2 QCD scaling violations of deep-inelastic structure functions[16] in the Q^2 range of HERA illustrated for an artificial input function $F_2(x,Q^2=3GeV^2) \sim \sqrt{x}(1-x)^3$ and compared with the statistical errors in a run of 250 pb^{-1} at $\sqrt{s}$ = 314 GeV.

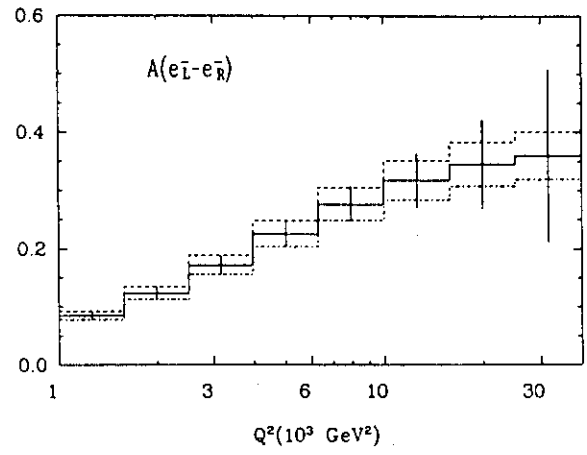

Fig. 3 Polarization asymmetry in $e^-_{L,R}p \rightarrow e^-X$ at $\sqrt{s}$ = 314 GeV integrated over x for $\sin^2\theta_w$ = 0.21 (dashed), 0.22 (full), 0.23 (dashed-dotted). The statistical errors are estimated for 100 pb^{-1} (e^-_R) and 50 pb^{-1}(e^-_L).

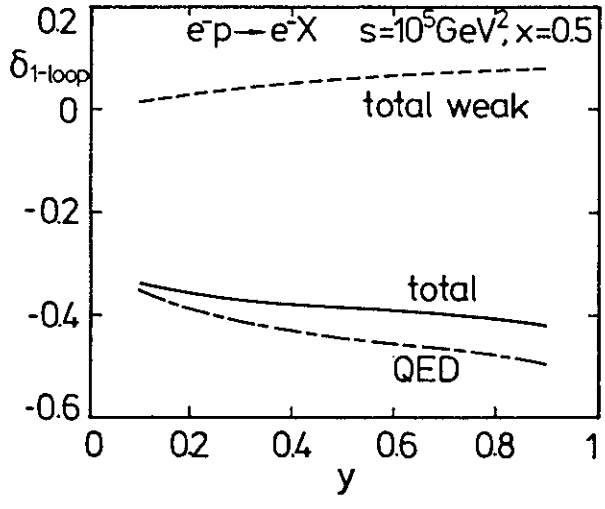

Fig. 4 Electroweak radiative corrections to the differential NC cross section[17]: $\delta_{1\text{-loop}}=(d\sigma_{1\text{-loop}}-d\sigma_{Born})/d\sigma_{Born}$ Input parameters are given in the test.

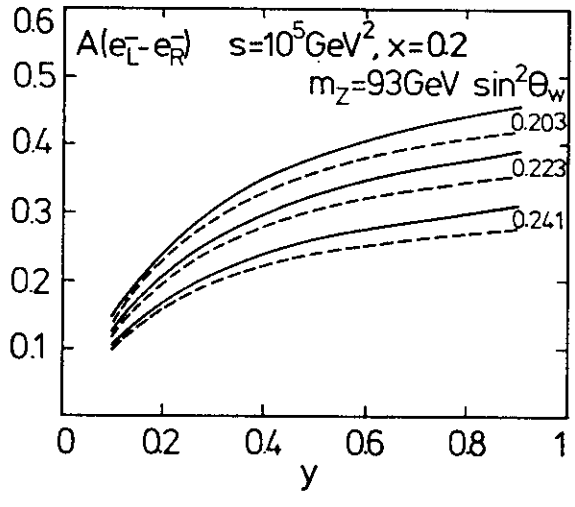

Fig. 5 Polarization asymmetries in $e^-_{L,R}p \rightarrow e^-X$ including electroweak radiative corrections (full curves) and in Born approximation (dashed curves) for three values of $\sin^2\theta_w$ corresponding to m_W = 83, 82 and 81 GeV, respectively.[17]

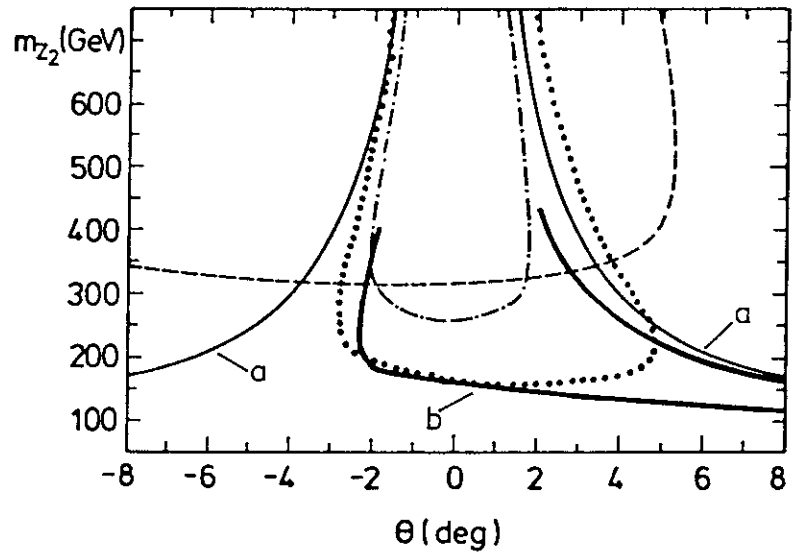

Fig. 6 Present-day bounds on the mass and mixing angle of a superstring-motivated neutral E_6 boson Z_2 (a) from W and Z mass measurements alone[47] and (b) from all NC data[45], in comparison with the sensitivity of NC asymmetries[50] at HERA. Indicated are the contours in (m_{Z_2}, θ) where $e_R^- - e_L^+$ (dashed), $e_L^- - e_R^-$ (dashed-dotted) and $e_R^- - e_R^+$ (dotted) deviate from the respective standard model values A = 0.52, 0.35 and 0.17 at x = 0.3, $Q^2 = 2 \times 10^4$ GeV^2 by $\delta A = 0.04$.

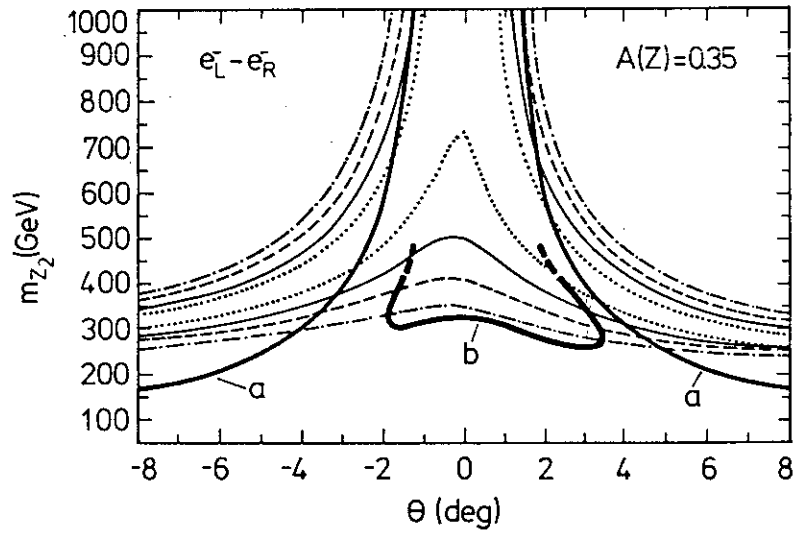

Fig. 7 Present-day bounds on the mass and mixing angle of a neutral boson associated with left-right symmetry (a) from m_W, m_Z measurements[47] and (b) from all NC data[45], in comparison with the sensitivity of a polarization asymmetry[52] at HERA. Shown are the contours in (m_{Z_2}, θ) where $A(e_L^- - e_R^-)$ at x = 0.3 and $Q^2 = 2 \times 10^4$ GeV^2 deviates by $\delta A = 0.02$ (dotted), 0.04 (full), 0.06 (dashed) and 0.08 (dashed-dotted) from the value A(Z) = 0.35 predicted in the standard model.

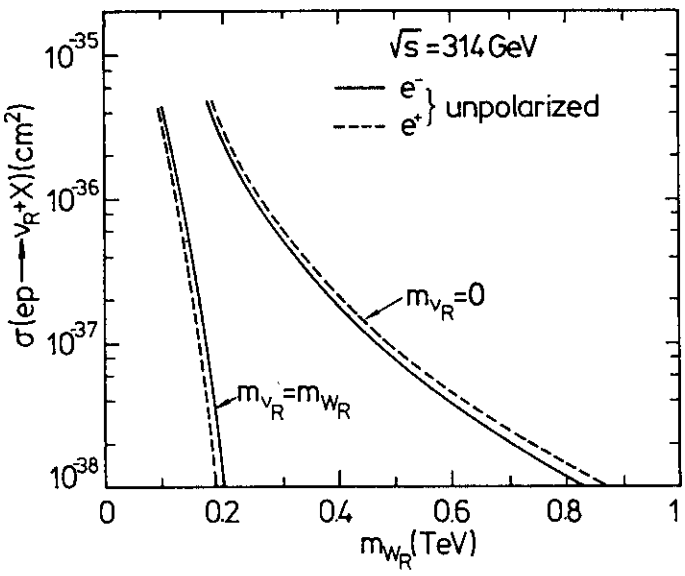

Fig. 8 Right-handed charged current cross sections at HERA for a heavy and a very light right-handed neutrino[7].

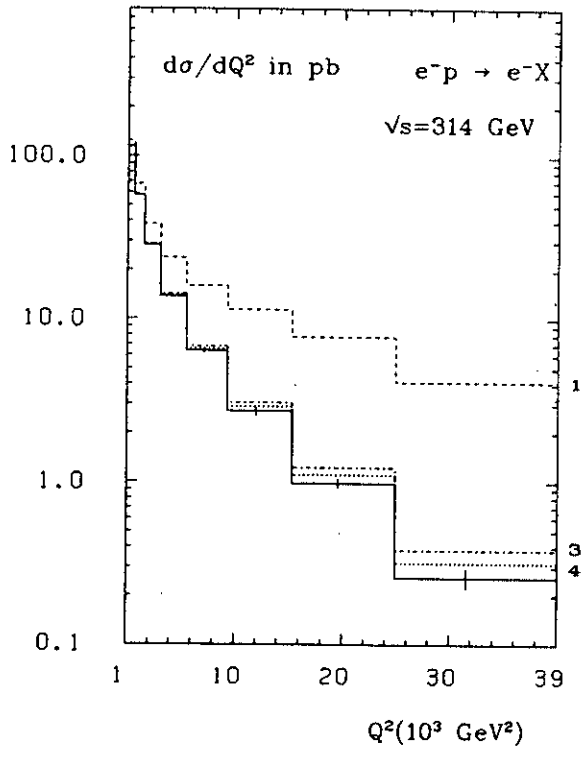

Fig. 9 Effects from LL-contact interactions (η_{LL} = +1) on the neutral current cross section[52] integrated over x for various values of the compositeness scale Λ_{eq} (TeV). The statistical errors on the standard model prediction (full curve) correspond to a run of 200 pb^{-1}.

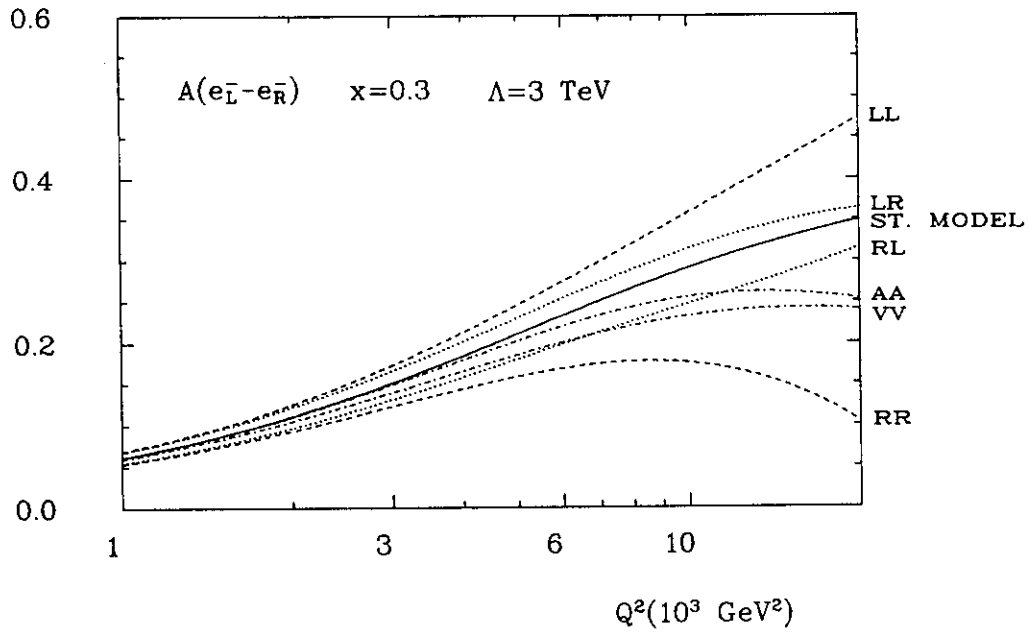

Fig. 10 Effects from contact interactions with different chiral structures (η = + 1) on a polarization asymmetry at HERA[52].

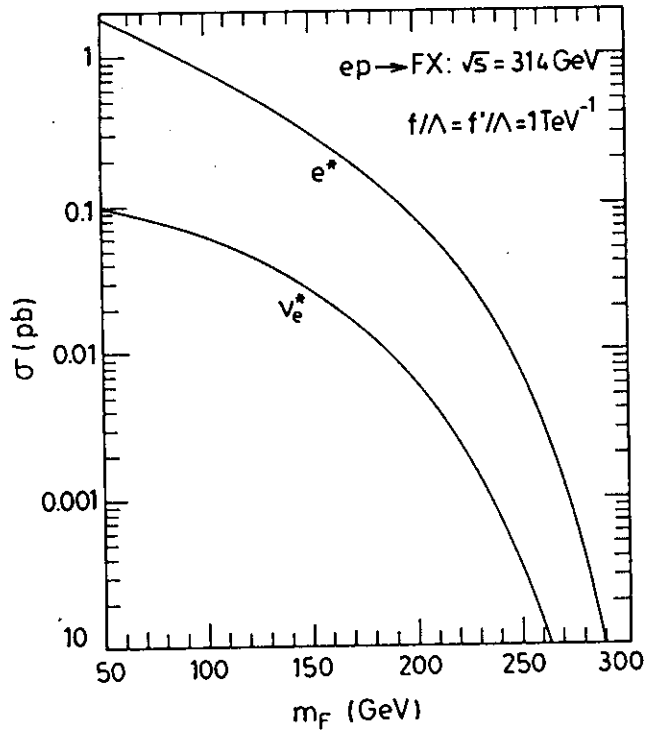

Fig. 11 Total cross sections at HERA for the production of excited electrons and neutrinos with magnetic transition couplings[58].

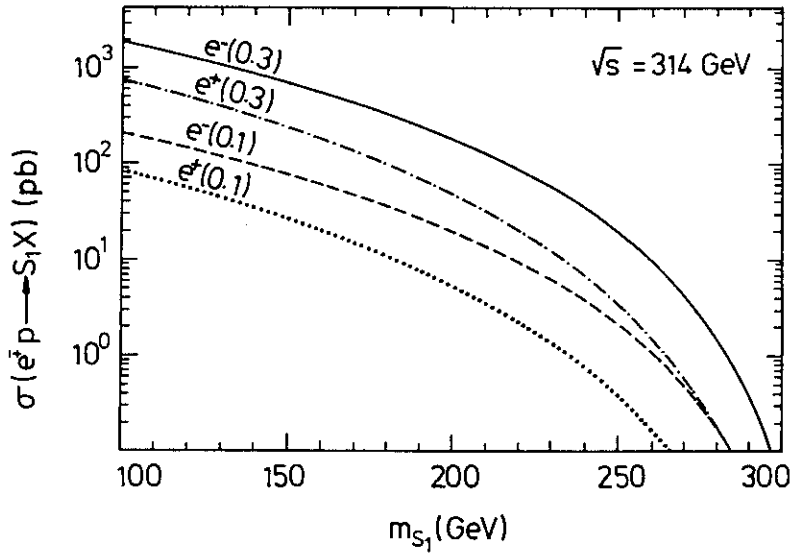

Fig. 12 Cross sections at HERA for the resonance production of the scalar leptoquark S_1 by e^-u and $e^+\bar{u}$ fusion and for two values of the coupling g_{1L} [63].

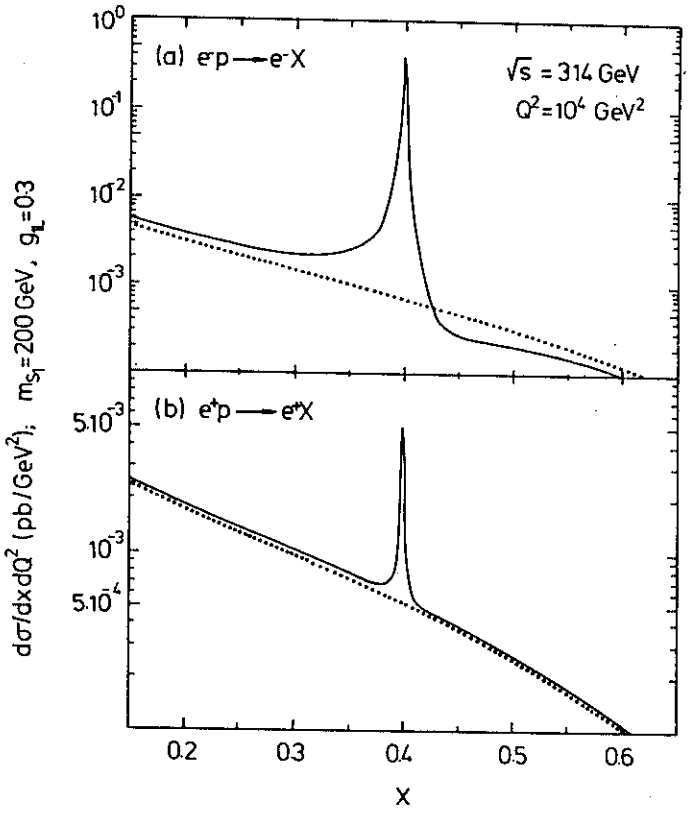

Fig. 13 Theoretical x-distributions in high Q^2 neutral current scattering at HERA if the scalar leptoquark S_1 exists with m_{S_1} = 200 GeV and g_{1L} = 0.3 (full curves) in comparison to the standard model predictions (dotted curves) [63].

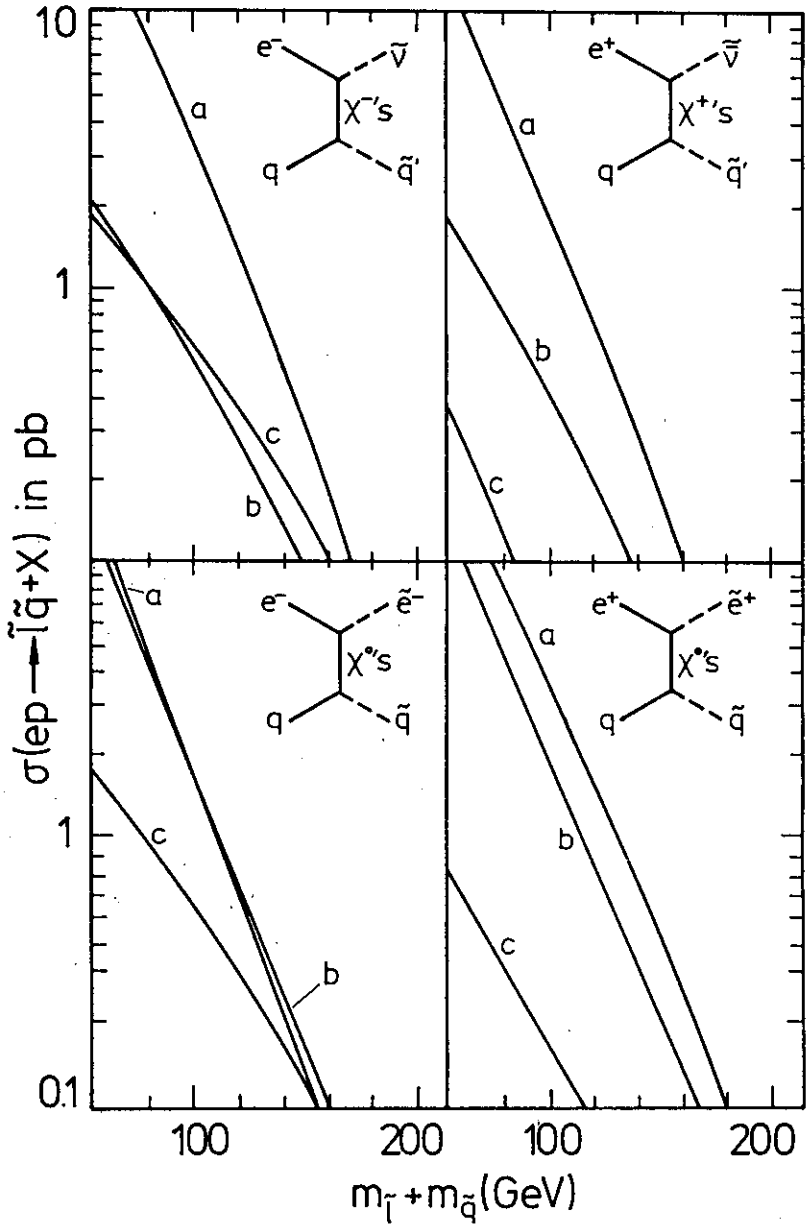

Fig. 14 Cross sections at HERA ($\sqrt{s}$ = 314 GeV) for the pair production of sleptons and squarks[73] with $m(\tilde{l}_L) = m(\tilde{l}_R)$ and $m(\tilde{q}_L) = m(\tilde{q}_R)$. The predictions a to c correspond to different chargino ($\chi_i^{\pm}$) and neutralino (χ_i^0) masses and mass eigenstates as given in Table 4.

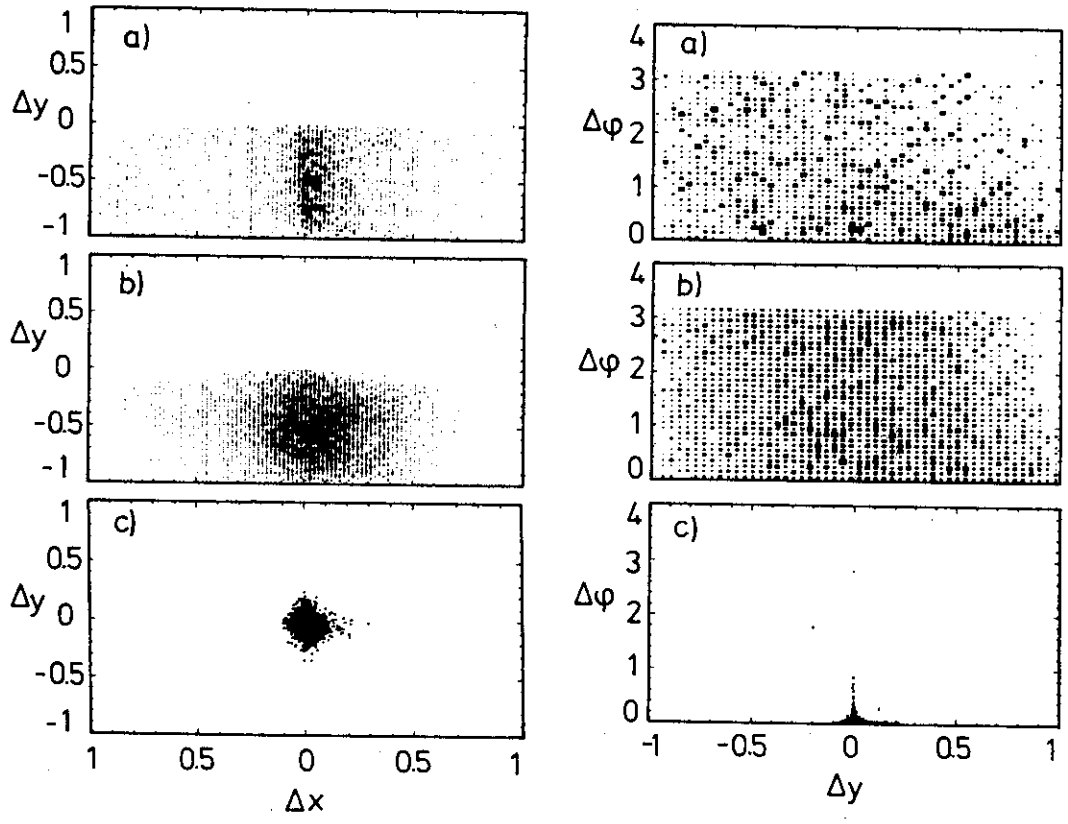

Fig. 15 Distributions in $\Delta y = y_q - y_e$ versus $\Delta x = x_q - x_e$ and in $\Delta\varphi = |\varphi_q - \varphi_e - \pi|$ versus $\Delta y = y_q - y_e$ for the following hypothetical SUSY events at HERA: $ep \rightarrow \tilde{e}\tilde{q}X$, $\tilde{e} \rightarrow e\tilde{\gamma}$, $\tilde{q} \rightarrow q\tilde{\gamma}$ with $m(\tilde{\gamma}) = 0$ and with (a) $m(\tilde{e}) = m(\tilde{q}) = 40$ GeV, (b) $m(\tilde{e}) = m(\tilde{q}) = 100$ GeV. The same distributions for conventional NC events, $ep \rightarrow eqX$, are shown in (c). Some detector smearing is taken into account[9].